FACULTY OF SCIENCE AND TECHNOLOGY

BACHELOR'S THESIS

Study programme / specialisation: **Biological Chemistry / Organic Chemistry**	The spring semester, 2023 Open
Author: **Lene Bjorøy Norevik**	
Supervisor at UiS: **Magne O. Sydnes** Co-supervisor: External supervisor(s):	
Thesis title: **Synthesis and photodecomposition of antibiotics containing ethanolamine and oxazolidine moieties.**	
Credits (ECTS): 20	
Keywords: **Antibiotics** **Photodecomposition** **Organic synthesis**	Pages: 33 + appendix: 41 Stavanger, 15.05.2023

Approved by the Dean 30 Sep 21
Faculty of Science and Technology

Abstract

Antimicrobial resistance is a leading cause of death globally and is on the rise. The discovery of new antibiotics is declining, and the synthesis of new scaffolds with decomposing properties is more important now than ever to combat the rise of antimicrobial resistance. The goal of this project was to synthesize photodecomposable antibiotics containing the ethanolamine moiety, and further modify this to the corresponding oxazolidine.

1-((2,5-Dichloro-4-nitrophenyl)amino)-3-phenylpropan-2-ol (**3a**) was successfully synthesized to a yield of 13%. Compound **3a** was used to synthesize 5-benzyl-3-(2,5-dichloro-4-nitrophenyl)oxazolidine (**4**) in a yield of 31%. Photodecomposition was conducted for compounds **3a** and **4**, and they were fully photodecomposed after approximately 24 hours as judged by ^{1}H NMR. Compounds **3a** and **4** have been submitted for biological testing and results are expected later this spring. Results from biological testing are therefore not included in this report.

Attempts were also made to synthesize 1-((2,6-dichloro-4-nitrophenyl)amino)-3-phenylpropan-2-ol (**3b**) using the appropriate aniline (**1b**) and (2,3-epoxypropyl)benzene (**2**). None of the reactions that were attempted were successful.

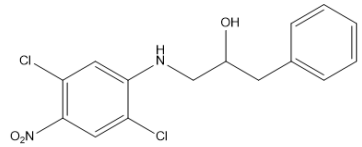

3a

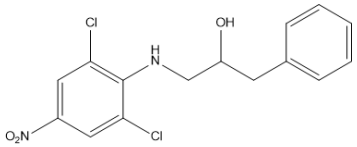

3b

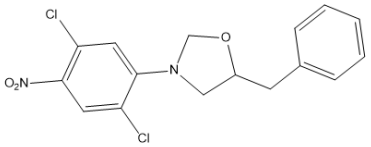

4

Table of Contents

Abstract **ii**
Abbreviations **1**
Acknowledgements **2**
1 Introduction **3**
1.1 The early discovery of antibiotics..……3
1.2 Antibiotic resistance and the dangers it poses.……..…….3
1.3 Green chemistry……...……..4
1.4 Recent advances in the field……..…….5
1.4.1 Photo-retro-aldol type reaction…….....…….5
1.4.2 Results previously found by the research group…….……6
1.4.3 The synthesis of a modified cephalosporanic-acid antibiotic…...……...8
1.4.4 Photoswitchable antibacterial agents……..……9
1.5 The excited state……...……...10
1.6 The aim of the project……...……...10
2 Results and discussion **12**
2.1 Attempted syntheses of ethanolamine derivatives using lithium bromide and various alcohols as solvent……12
2.2 Attempted syntheses of 1-((2,6-dichloro-4-nitrophenyl)amino)-3-phenylpropan-2-ol (**3b**) using LPDE and LPEtOAc…….……...14
2.3 Syntheses of 1-((2,5-dichloro-4-nitrophenyl)amino)-3-phenylpropan-2-ol (**3a**) using LPDE and LPEtOAc……16
2.4 Synthesis of 5-benzyl-3-(2,5-dichloro-4-nitrophenyl)oxazolidine (**4**)…….19
2.5 Photodecomposition studies……20
2.6 Summary of results……..22
2.7 Further research……...22
3 Concluding remarks **24**
4 Experimental sections **25**
4.1 General information……..……...25
4.2 Synthesis procedures…….……..25
5 References **31**
6 Appendix **34**

Abbreviations

ACN	Acetonitrile
AMR	Antimicrobial resistance
DCE	1,2-Dichloroethane
DCM	Dichloromethane
Et_2O	Diethyl ether
EtOAc	Ethyl acetate
EtOH	Ethanol
EWG	Electron withdrawing group
h	Hour(s)
HMBC	Heteronuclear Multiple Bond Correlation
HRMS	High resolution mass spectrometry
HSQC	Heteronuclear Single Quantum Coherence
Hz	Hertz
ISC	Intersystem crossing
LPDE	Lithium perchlorate-diethyl ether
LPEtOAc	Lithium perchlorate-ethyl acetate
MeOH	Methanol
NMR	Nuclear magnetic resonance
pet. ether	Petroleum ether
PMA	Phosphomolybdic acid solution
ppm	Parts per million
R_f	Retention factor
rt	Room temperature
S_0	Singlet state
S_1	Excited singlet state
STP	Sewage treatment plant
T_1	Triplet state
TFE	2,2,2-trifluoroethanol
TLC	Thin-layer chromatography
UV	Ultraviolet
UV-vis	Ultraviolet-visible

Acknowledgements

I would like to thank my supervisor Professor Magne O. Sydnes for great help and guidance during my bachelor's project. I would also like to give a special thanks to Susana E. Duran for teaching me all the techniques I needed in the lab, and for explaining and discussing results and theories with me. I would also like to thank the rest of my research group Maélys, Stephanie, Zeynep, Siri and Liza for keeping morale high and helping me whenever I had a question. I would also like to thank my significant other, Halvor F. Sundal, for letting me complain whenever an experiment did not go as planned, for being a great conversation partner, both related to and unrelated to the project, and for supporting and motivating me to do my absolute best.

1 Introduction

1.1 The early discovery of antibiotics

Antibiotics are chemical substances made by or derived from living organisms that possess the ability to stump growth or kill certain bacteria. In modern times, antibacterial agents can also be made synthetically, and does not have to be produced by living organisms directly[1].

The first antibiotic, penicillin, was an accidental discovery by Alexander Fleming in 1928[1,2]. Fleming was culturing *Staphylococcus* variants, and the cultured plates were set aside. The plates were exposed to air and were eventually contaminated by surrounding micro-organisms. One of the micro-organisms was a mold that seemed to force the *Staphylococcus* colonies to undergo lysis. Further testing was done on subcultures of this mold, and it was found that the broth of the mold contained inhibitory, bactericidal and bacteriolytic properties against many common pathogenic bacteria[1,2].

Although the first antibiotic was discovered in 1928, it took numerous years before the potential for antibiotics in regard to fighting bacterial diseases was acknowledged, and production was increased. Most classes of antibiotics were discovered between 1940-1960, and large-scale production of antibiotics was developed in the 1940s[1].

1.2 Antibiotic resistance and the dangers it poses

Penicillin was prescribed to World War II soldiers to treat bacterial infections in the 1940s. Penicillin was successful at treating these bacterial infections for a while, however, in the 1950s penicillin resistance had arisen and started to become an issue. Due to this, new variants of penicillin and new classes of antibiotics, were developed and introduced in the medical field[3]. These classes were based on a few scaffolds, the β-lactams, tetracyclines, sulfonamides, cephalosporins, quinolones and macrolides to give a few examples[3,4]. As antimicrobial resistance (AMR) arose, new generations based on these scaffolds were designed and introduced to combat bacteria that had become resistant to the previous generations[4]. Bacteria kept developing resistance to the new generations of antibacterial agents, and a study from 2022 estimated that 1.27 million deaths were directly caused by AMR, while 4.95 million deaths were associated with AMR in 2019. AMR is now a leading cause of death globally, with the most dire consequences in low-resource areas[5].

The rise of AMR is a result of overuse and misuse of antibiotics, including a lack of new drug development, and studies have shown that antibiotic prescriptions are incorrect in 30% to 50% of the cases[3]. There is a lack of new drug development for several reasons. Antibiotics are usually curative and only meant for short time use. Due to this, antibiotics are less profitable than medicines meant for chronic conditions such as diabetes, where continued medicinal use is necessary. In addition to this, antimicrobial use is not recommended unless absolutely necessary, so if a new antibiotic is introduced on the market, physicians would rather prescribe already used antibiotics, and spare the new antibiotics for when nothing else works in fear of promoting AMR[3]. Lastly, since most new antibiotics have been based on the same few scaffolds

and many new generations of antibiotics has been made for each scaffold, antibiotic discovery has dwindled, and new generations are getting more and more difficult to develop[3,4].

Antibiotics are used not only in human and veterinary medicine to prevent and treat bacterial infections, but also in aquaculture for fish farming and in agriculture to promote more rapid growth in livestock[3,6]. Due to lack of regulations regarding the use of antibiotics in certain areas of the world (mostly in low- and middle-income countries), antimicrobials are often misused and overused in these areas[5,7]. Treating livestock with antimicrobials improves the overall health in animals and produces larger yields, which helps farmers produce a higher-quality protein for the consumers[3], and according to a study published in 2019, 73% of all antibiotics used are used in animals raised for food[7]. After their use in medicine, fish farming, agriculture and other fields, antibiotics are released into the environment in their active form[6], and up to 90% of antibiotics given to livestock or used for human or veterinary medicine are excreted in urine and stool in their biologically active form or as active metabolites[3,8]. Antibiotics used in animals raised for food enters the environment when manure is applied to fields as fertilizer, and may end up in soil, sediments or ground water[6]. Human excreta containing only partially metabolized antibiotics are discharged into the hospital sewage system or municipal waste water, which then flows to a sewage treatment plant (STP)[6]. The sewage treatment process and other waste management systems are only partially effective at removing antibiotics, and antibiotic residues and antibiotic resistant bacteria can be detected in the effluent of STPs, sediments, soils and different aquatic environments, such as waste water, ground water, sea water and even drinking water[6,8,9].

Many antibiotics persist in nature for a long time, and many types of antibiotics are not biodegradable[6,8,9]. Certain antibiotics degrade easily, such as the β-lactams, while other persist for a longer time and accumulates in a cocktail of different antibiotics, such as fluoroquinolones and tetracyclines[8]. The concentrations of antibiotics in the environment are usually much lower than what is prescribed for medicinal use, however, antibiotic concentrations exceed the thresholds for development of antibiotic resistance in many aquatic environments, such as in surface water, groundwater, wastewater and wastewater treatment plants/STPs[6,8].

The discovery of antibiotics has saved millions of lives from bacterial infections, and even made it possible for people and animals to undergo invasive surgeries, chemotherapy, and other immune shattering procedures. Antibiotics have successfully treated and prevented bacterial infections in patients with cancer, in need of joint replacements or organ transplants, patients with chronic diseases and much more. Antibiotics have successfully extended the human life span, however all of this is now at a risk due to the increase of AMR[3,5,7].

1.3 Green chemistry

A large part of the antimicrobial resistance crisis can be traced back to the bioaccumulation of active antimicrobial agents in the environment[3,6,10,11]. Minute concentrations of several antimicrobials exist at the same time in the environment, and promote resistance through mutagenesis and horizontal gene transfer[6,10,12]. One major method of combating the AMR crisis is to develop antimicrobial agents that become inactivated after doing their work in a patient.

Kümmerer introduced the concept “benign by design” in 2007 to describe chemicals that degrade in the environment after use. Such chemicals could aid in the decrease of AMR by being broken down before bacteria can develop resistance[10,11].

It has long been assumed that antimicrobials and other pharmaceuticals need to be strong and stable structures to be successful in the pharmaceutical industry[10,11], especially if they are to be taken orally and withstand the acidity in the stomach, which most antimicrobials are[10]. However, new structures need to be made that are strong enough to do their work on a patient (whether they are taken orally, intravenously or in another way), but weak enough to degrade when they are excreted to the environment. The products of the decomposition also need to be inactive and non-toxic, and preferably also easily further degraded[10,11]. Many such antimicrobials are under active research, with research groups focusing on temporary light-activation[12,13] and photodecomposition[10,14–16].

1.4 Recent advances in the field

1.4.1 Photo-retro-aldol type reaction

Wan and Muralidharan discovered a photo-retro-aldol type reaction while researching the photodecomposition of phenethyl alcohols with *p*- and *m*-substituted nitro-groups and varying substituents (R) in position 1 (Scheme **1**). The reaction was observed at different pH-values, and resulted in a heterolytic cleavage of the benzylic C-C bond[17,18].

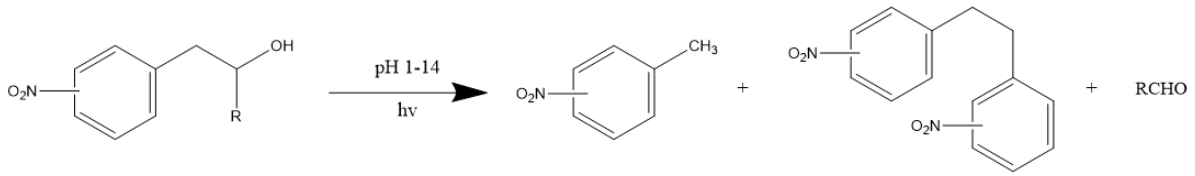

Scheme 1. Photolytic cleavage of benzylic C-C bond in nitrophenethyl alcohols. R = H, Ph[17–19].

1-phenyl-substituted alcohols reacted via the photo-retro-aldol process at various pH-values with conversions from 30%-60%[17,19]. Irradiation of the singlet ground state (S_0) by UV-light yields the excited singlet stage (S_1), which then undergoes intersystem crossing (ISC) to the reactive triplet stage (T_1)[16,17] (Scheme **2**). The mechanism suggests the retro-aldol pathway of the reactive triplet stage by removal of a proton by water or hydroxide. This gives an aldehyde and *p*-nitrobenzyl carbanion, which reacts further to give *p*-nitrotoluene and 4,4’-dinitrobibenzyl[17,19].

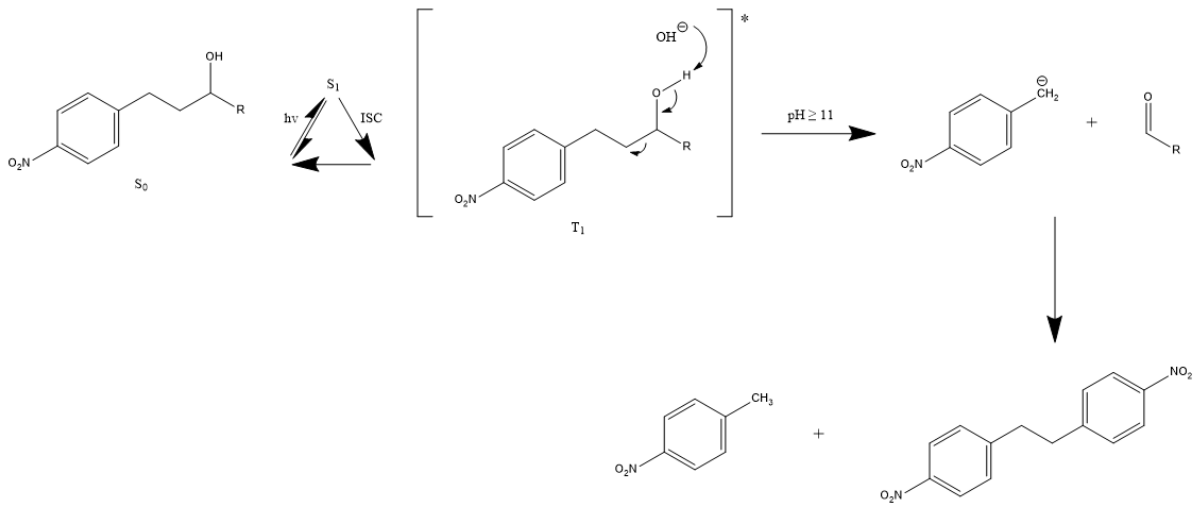

Scheme 2. Summary of photo-retro-aldol type reaction through irradiation of the ground state (S_0) to form the singlet excited state (S_1), which undergoes intersystem crossing (ISC) to form the reactive triplet stage (T_1)[17,19].

1.4.2 Results previously found by the research group

The development of a new antibiotic containing a photodegradable unit was inspired by the work on the photo-retro-aldol type reaction by Wan and Muralidharan[16–19]. A similar benzylic alcohol was incorporated into biologically active molecules that would undergo photofragmentation into biologically inactive molecules[16]. The result was 1-(arylamino)-3-arylpropan-2-ol derivatives with an aromatic ring on each side of the chain and a nitro group in the *para*- or *meta*-position on either ring (Figure **1**)[15,16,19].

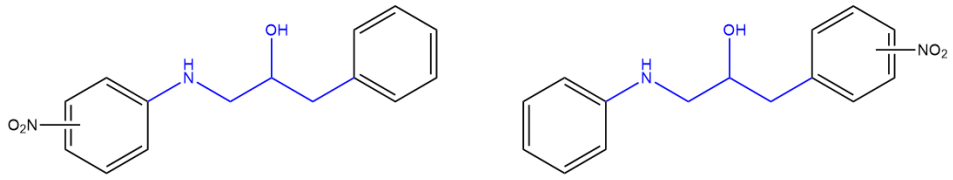

Figure 1. Derivatives of 1-(arylamino)-3-arylpropan-2-ol with the ethanolamine scaffold outlined in blue.

The first few model compounds were synthesized by Eikemo *et al*. using an aniline with a nitro group in the *p*- or *m*-position and (2,3-epoxypropyl)benzene (**2**) and a microwave-assisted epoxide ring opening following conditions by Lindsay and co-workers[19,20] (Scheme **3**).

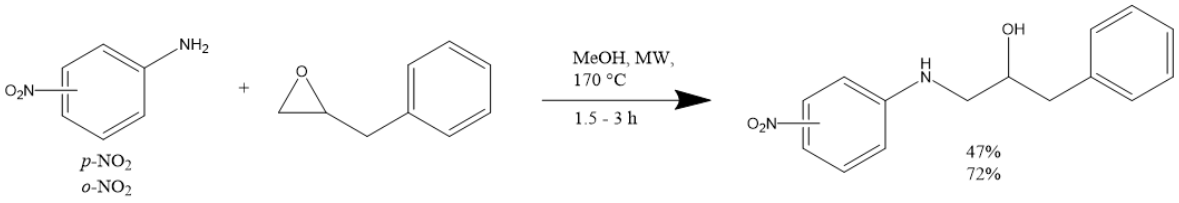

Scheme 3. Microwave-assisted synthesis of the ethanolamine scaffold[16,19].

The *para*-substituted ethanolamine was synthesized in good yield (72%), but the *ortho*-substituted product was only produced by a 47% yield. The yield of the *ortho*-substituted

ethanolamine was increased to 64% when the reaction was performed in 5 M LPDE, a procedure reported by Heydari and co-workers[19,21].

The synthesized products were photodecomposed at varying pH-values to evaluate the rate of decomposition, if the decomposition is pH-dependent, and to find the decomposition mechanism. The Photodecomposition was run for two hours according to the procedure by Wan and Muralidharan[17,19]. 1-((4-nitrophenyl)amino)-3-phenylpropan-2-ol (**5)** was photolyzed in acetonitrile and water (7:3, ACN/water) (Scheme **4**). Irradiation excites compound **5** into its excited singlet state, which undergoes intersystem crossing into its triplet state, which allows the compound to decompose to form *N*-methyl-*p*-nitroaniline and phenylacetaldehyde[16,19]. Photoinduced *N*-demethylation has been proven to occur for anilines[22,23], and *N*-demethylation of *N*-methyl-*p*-nitroaniline yields *p*-nitroaniline and formaldehyde (Scheme **4**, a). The phenylacetaldehyde can oxidize in the presence of oxygen to form phenylacetic acid (Scheme **4**, b), or it can react in a Norrish type I photocleavage reaction to form formaldehyde and a benzyl radical, which is oxidized to benzaldehyde in the presence of oxygen (Scheme **4**, c). Benzaldehyde can further oxidize to benzoic acid (Scheme **4**, d). Furthermore, phenylacetic acid can undergo cleavage to form benzaldehyde, formaldehyde and formic acid (Scheme **4**, e)[16,19].

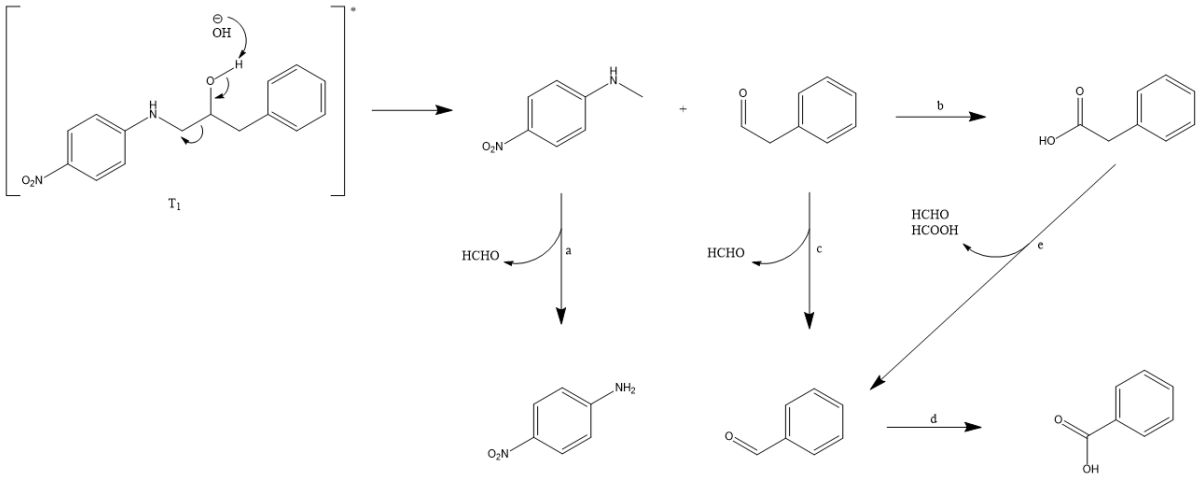

Scheme 4. The mechanism for the photodecomposition of compound **5**[16,19].

A photodecomposition was also performed on the other ethanolamine model compounds, however, the decomposition proved to be most successful when the nitro-group is in the *para*-position on the aniline. This ethanolamine, compound **5**, had a 32% degradation at pH 7 and 100% degradation at pH 11 and 13[19].

With the model compounds synthesized and the degradation mechanism established, many more ethanolamine derivatives were synthesized, tested for biological activity, and photodegraded (Figure **2**). All ethanolamine derivatives were synthesized in a 5 M LPDE solution at 40 °C[15,16,19]. Compounds **6a**-**6k** were screened for biological activity against laboratory strains of Gram-positive and Gram-negative bacteria, including *Escherichia faecalis*, *E. coli*, *Pseudomonas aeruginosa*, *Staphylococcus aureus*, *S. agalacticae*, and *S. epidermidis*, and compounds **6a**-**6d** showed promising biological activity against two or more of the strains

tested. Compounds **6a** and **6d** showed antibacterial activity with a minimum inhibitory concentration (MIC) of 6.3 μM against *S. agalacticae*[15,16,19]. The biologically active compounds, compounds **6a-6d**, were subjected to photodecomposition at pH 8 and pH 13. Compounds **6a-6c** decomposed 100% at pH 13, while compound **6d** decomposed 56%. Compounds **6b** and **6d** decomposed 100% at pH 8, while compounds **6a** and **6c** decomposed 25% and 19%, respectively. It was also proved that not all of the compounds followed the same photodegradation mechanism as compound **5**[16,19].

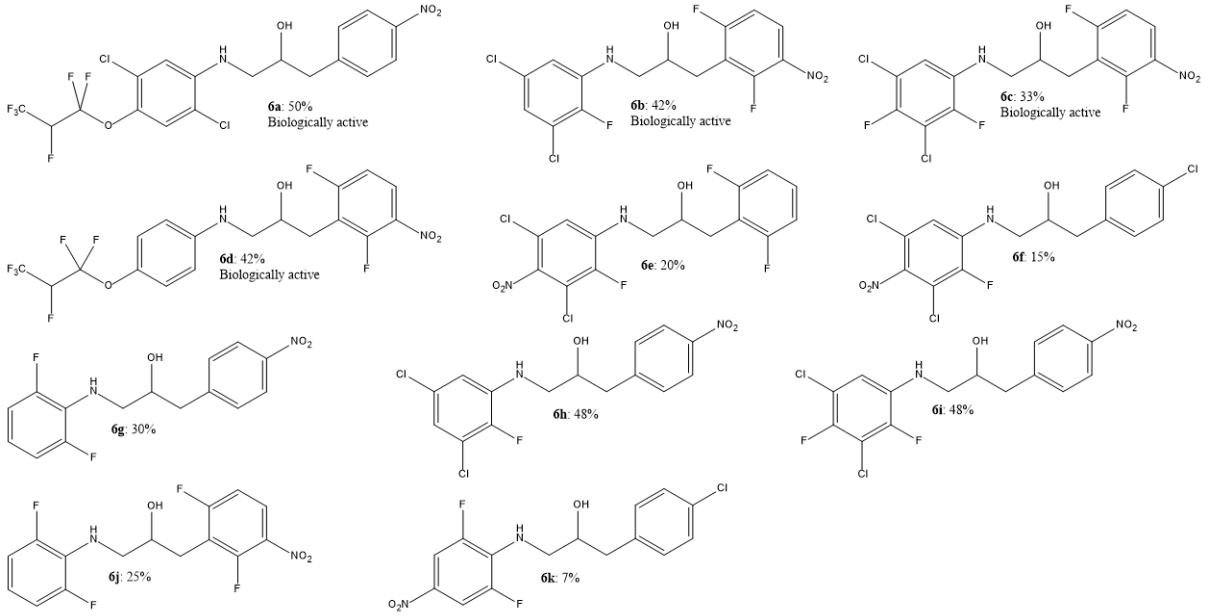

Figure 2. Ethanolamines reported by Eikemo *et al*. Four of the compounds showed promising biological activity[15,16,19].

1.4.3 The synthesis of a modified cephalosporanic-acid antibiotic

The first example of an antibiotic with the ability to photodecompose was reported by Mobashery and co-workers in 2000[10,14]. The group synthesized a modified antibiotic based on the cephalosporanic acid scaffold which, in a matter of hours, undergoes light induced destruction of its β-lactam moiety[10,12,14] (Scheme **5**). The antibiotic was modified to contain a hydrazine-protected *o*-nitrobenzylcarbamate moiety. The *o*-nitrobenzylcarbamate is cleaved off when the chemical is irradiated by UV-light. The hydrazine, which is a super nucleophile, then reacts with the lactam carbonyl, cleaving its C-N bond, which destroys the molecules antibacterial properties[10,14]. The modified cephalosporanic acid compound was also tested for antibacterial properties against several lab strains of bacteria, and, although it showed antibacterial activity against all the strains tested, it showed more activity against the Gram-positive bacteria than the Gram-negative bacteria that were tested[14].

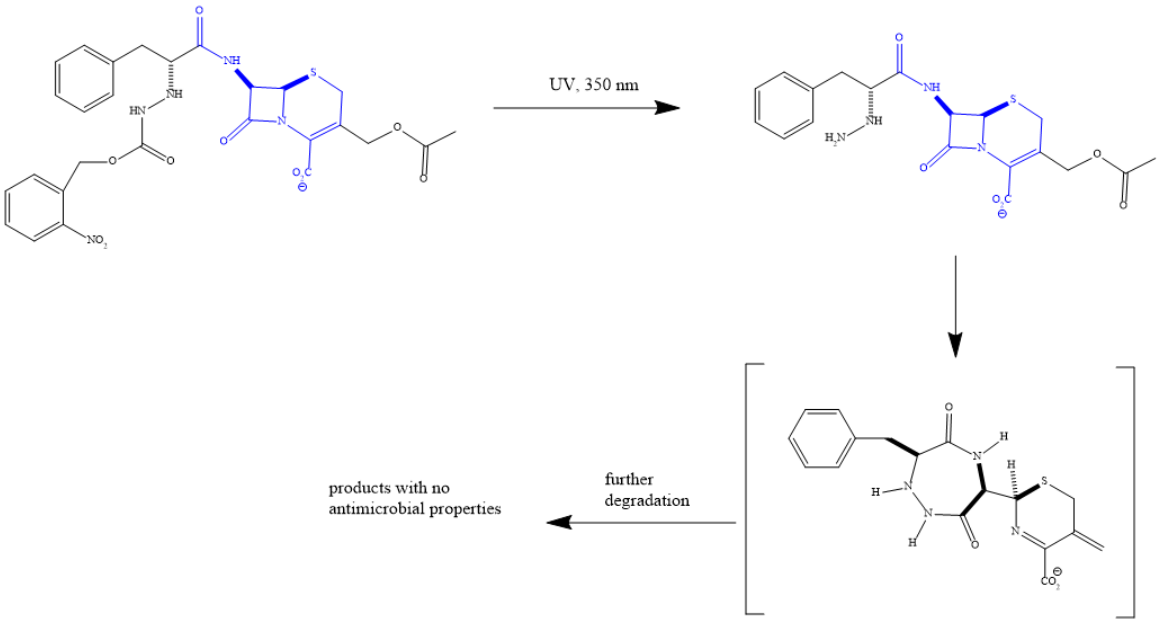

Scheme 5. Summary of the photodecomposition of the modified cephalosporanic acid prepared by Mobashery and co-workers. The cephalosporin scaffold is outlined in blue[10,14].

1.4.4 Photoswitchable antibacterial agents

Feringa and co-workers took a different approach by incorporating biological photoswitches into biologically active antimicrobials[12,13]. The research group based their antimicrobials on the quinolone scaffold[12,13], which is a widely used antimicrobial group with a broad spectrum[12]. The quinolones are bactericidal by binding to DNA gyrase and inhibiting DNA replication in bacteria[12,24]. Clinically used quinolones often contain a piperazine moiety, however, this was exchanged for an aryldiazo moiety, which renders the compound photoresponsive and able to switch between its *cis* and *trans* isomers (Scheme **6**). The compound has a *trans* configuration in its less active state, however, irradiation by UV-light converses the compound into its *cis* isomer which has antimicrobial properties. Visible light and/or ambient temperatures lead to the conversion of the *cis* isomer back to its *trans* isomer and renders the compound inactive. Reversible switching between the *trans* and *cis* isomers could be performed for three consecutive cycles before causing significant fatigue. Biological testing on the *cis* isomer also proved that it showed antimicrobial activity towards both Gram-positive and Gram-negative bacteria, thus retaining its broad spectrum of antimicrobial activity[12].

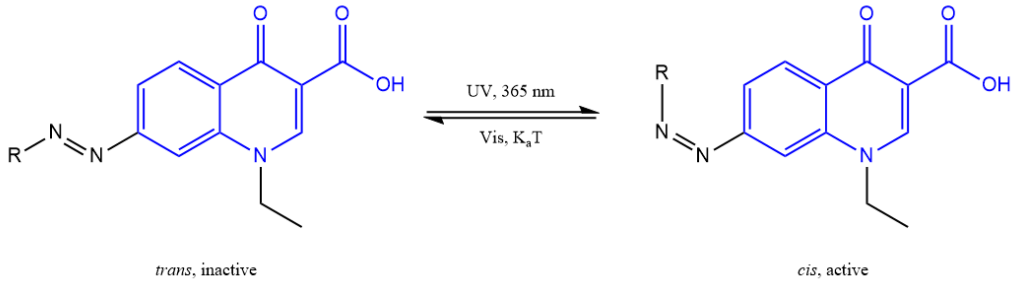

Scheme 6. *Cis* isomer (active) and *trans* isomer (inactive) of the aryldiazo-containing quinolone by Feringa and co-workers. The quinolone scaffold is outlined in blue. R = 3-Methyl-4-methoxyphenyl[12].

1.5 The excited state

All the reactions in the previous chapter were initiated by electromagnetic radiation, more specifically UV-light. The initiation of a chemical reaction by light is known as photochemistry[25], and photodecomposition is an example of a photochemical reaction[25,26]. Absorption of energy by a molecule is known as excitation. A molecules lowest energy state is known as the ground state (S_0), but if a molecule absorbs electromagnetic energy at a high enough level, the electrons in the molecule will be raised to a higher energy excited state[25,26]. If the absorption of energy is high enough, usually in the UV or visible light area of the spectrum, the energy of the molecules excited state might be comparable to the molecules dissociation energy, and the molecule could decompose[25].

When a molecule is excited, one or more electrons move from a bonding or non-bonding molecular orbital (σ, π, n) to an antibonding orbital (σ*, π*). When this happens, the excited electron may take a paired electron spin configuration, which is known as the singlet state (S_1), or a parallel electron spin configuration, which is known as the triplet state (T_1)[19,25]. For the excited electron to be able to take the triplet state, the molecule needs to undergo intersystem crossing (ISC) from the singlet state. When in the excited state, several things may happen; the excitation energy may be emitted from the singlet state in the form of fluorescence, followed by a vibrational cascade down to the ground state ($S_1 \rightarrow S_0$), the energy can be emitted from the triplet state as phosphorescence, followed by a vibrational cascade down to the ground state ($T_1 \rightarrow S_0$), or there could be an internal conversion from $S_1 \rightarrow S_0$ followed by a vibrational cascade down to the ground state[19,25,26]. If the energy in the excited state is sufficient, a photochemical reaction may take place instead, such as the photo-retro-aldol type reaction or aryldiazo *trans* to *cis* isomerization[12,13,17,18].

1.6 The aim of the project

As previously discussed, the rise of AMR is a large threat to human and animal health[3,5,7], and using degradable antimicrobials is a good way to remove antibiotics from the environment to help halt the development of AMR[10,11]. The aim of this project is to synthesize photodegradable antimicrobial agents containing ethanolamine and oxazolidine moieties. AMR bacteria contain mechanisms for detoxifying antimicrobials based on old scaffolds, however, new scaffolds

would require new detoxifying mechanisms, which means bacteria will not be able to inactivate antimicrobial agents containing new scaffolds[4,10]. The development of the ethanolamine scaffold was done by Eikemo *et al*., and was inspired but the photo-retro-aldol type reaction reported by Wan and Muralidharan[15–19]. This project is a continuation of that work to find biologically active and photodegradable ethanolamine and oxazolidine derivatives.

The focus of this project has been to synthesize and study the photodecomposition of 1-((2,5-dichloro-4-nitrophenyl)amino)-3-phenylpropan-2-ol (**3a**), 1-((2,6-dichloro-4-nitrophenyl)amino)-3-phenylpropan-2-ol (**3b**), and 5-benzyl-3-(2,5-dichloro-4-nitrophenyl)oxazolidine (**4**). The starting materials for the ethanolamines are their respective anilines, 2,5-dichloro-4-nitroaniline (**1a**) to synthesize compound **3a** and 2,6-dichloro-4-nitroanilie (**1b**) to synthesize compound **3b**, and (2,3-epoxypropyl)benzene (**2**). A small modification can be done using the relevant ethanolamine and formaldehyde to yield the corresponding oxazolidine. The oxazolidine moiety is an essential component in many biologically active agents[27], and many oxazolidine derivatives and analogs have been proved to show antimicrobial activity against Gram-positive and Gram-negative bacteria[27,28]. Compound **4** is therefore a good candidate to test for antimicrobial properties, and relevant to synthesize.

The nitro-group and its position on the ethanolamines somewhat determines the rate of photodecomposition[16,19,29]. Eikemo *et al*. proved this in a study of the photodecomposition mechanism of the ethanolamine model compounds, where having the nitro-group in *para*-position on the aniline resulted in a higher rate of decomposition than when the nitro-group was in the *meta*-position on the aniline or in the *para*- or *meta*-position on the epoxide[16,19]. Wan *et al*. studied several *p*-nitrobenzyl and *m*-nitrobenzyl systems in 1987 and found that many of these systems are photolabile in aqueous solutions due to the nitro-group[29].

2 Results and discussion

2.1 Attempted syntheses of ethanolamine derivatives using lithium bromide and various alcohols as solvent

Attempts were made to synthesize compounds **3a** and **3b** using a Lewis-acid epoxide ring opening with LiBr as the Lewis-acid and EtOH, MeOH, or 2,2,2-trifluoroethanol (TFE) as the solvent (Scheme **7**). The idea was that the lithium ion would function as a Lewis-acid catalyst by binding to the epoxide and opening the ring, making the epoxide more susceptible to a reaction with the appropriate aniline[21,30]. However, the reaction led to an epoxide ring opening with the solvent as evident by ^{1}H NMR (Figure **3**), and neither aniline **1a** nor **1b** reacted with the epoxide. The anilines are very poor nucleophiles, and the conjugate acid of *p*-nitroaniline has a p*K*a value of 1.0[31]. The presence of electron withdrawing groups, such as in compounds **1a** and **1b**, further lowers the p*K*a values, making the compounds more inferior as nucleophiles[32,33]. The inferior nucleophilicity of the anilines explains why the reactions result in nucleophilic addition of the alcohol solvents to the epoxide.

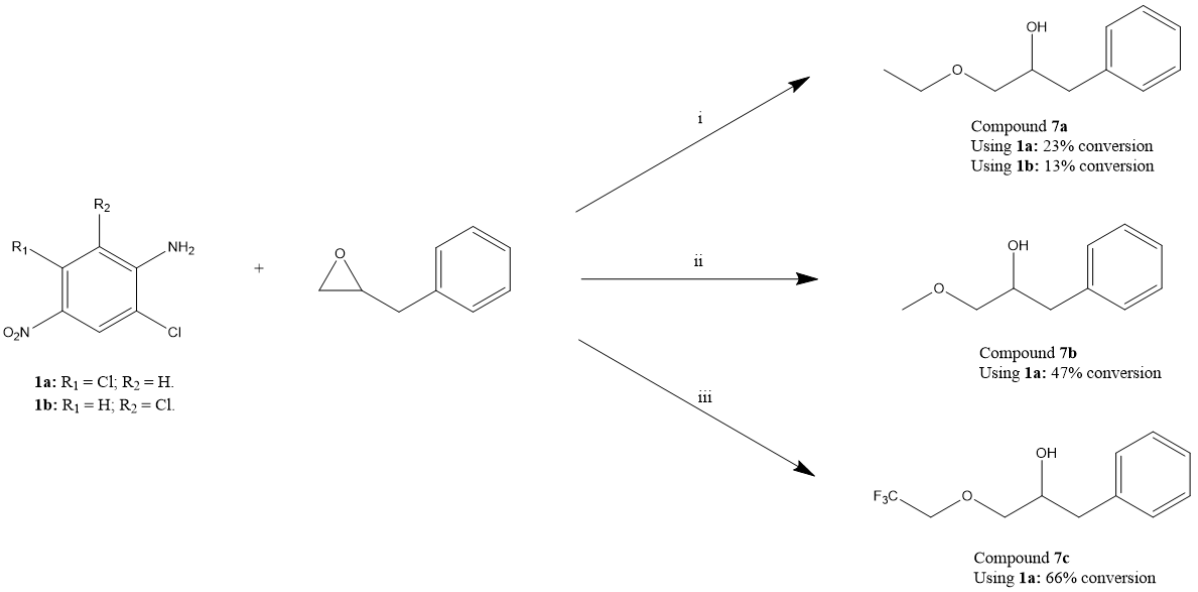

Scheme 7. Synthesis of compounds **7a-7c**. Reagents and conditions: (i) EtOH, reflux; (ii) MeOH, reflux; (iii) TFE, reflux.

As seen in Scheme **7**, the reactions using EtOH as solvent had a conversion of 23% when compound **1a** was used and 13% when compound **1b** was used. Compound **7b**, using MeOH as solvent, had a conversion of 47%, and compound **7c**, using TFE as solvent, had a conversion of 66%.

The difference in reactivity of the two reactions that gave compound **7a** can most likely be explained by the difference in concentration the reactions were run at. The reaction using compound **1a** was conducted at a concentration of 0.6 M, and the reaction using compound **1b** was run at a concentration of 0.2 M. In a reaction mixture with a high concentration, less solvent is used, which means the reactants are in a more restricted mixture and therefore more likely to come across other reactants. In reaction mixtures with lower concentrations, there is more

solvent for the reactants to spread throughout, and it is therefore less likely that reactants will react[34].

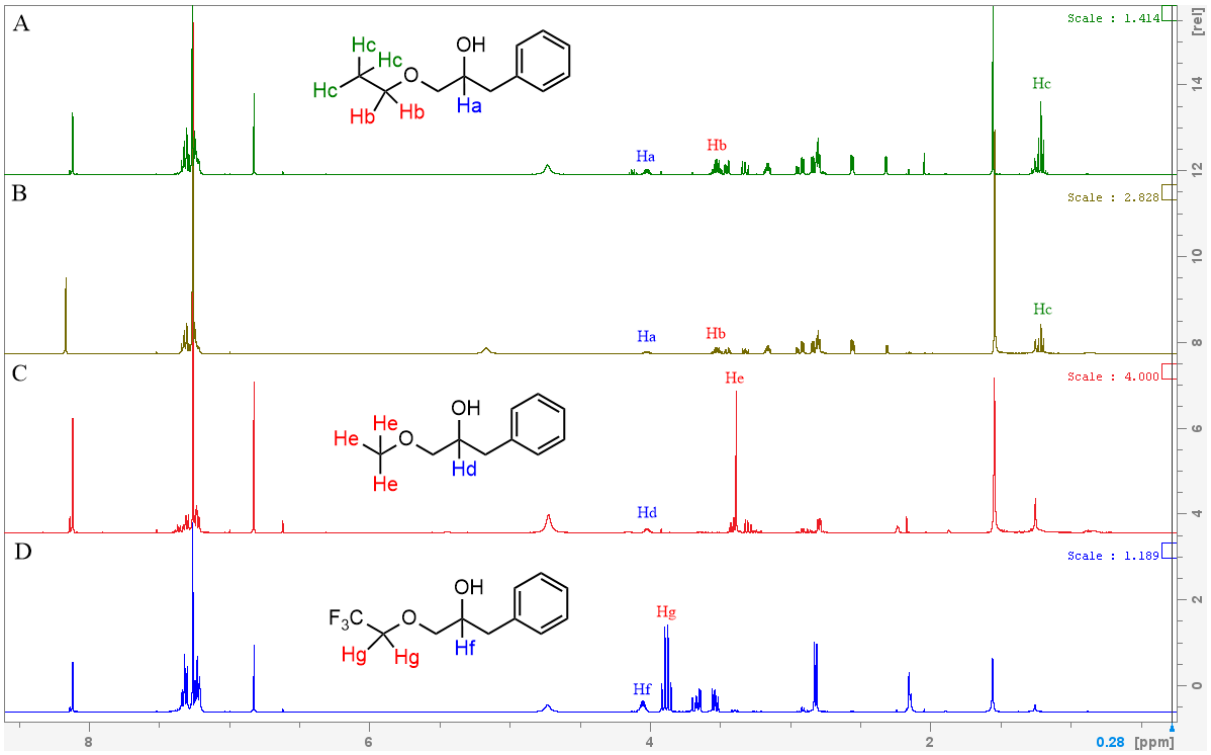

Figure 3. ^{1}H NMR spectra displaying crude products containing compounds (A, using compound **1a**, and B, using compound **1b**) **7a** and (D) **7c**, and most pure fraction of (C) **7b**.

Compounds **7a** and **7b** have previously been synthesized by Kim and co-workers in 2004 (Scheme **8**)[35]. Kim and co-workers used the same principle with a Lewis-acid epoxide ring opening and the appropriate alcohol, however, instead of LiBr as the Lewis-acid, the research group used indium(III) chloride as a Lewis-acid and catalyst. The reactions used to synthesize compounds **7a** and **7b** were run at 50 °C for 22 h and 37 h, respectively. The compounds were synthesized in good yields, with 64% yield for compound **7b** and 52% yield for compound **7a**. Both reactions gave two products; compound **7b** and 1-chloro-3-phenylpropan-2-ol (21% yield) when MeOH was used, and compound **7a** and 2-ethoxy-3-phenylpropan-1-ol (< 9% yield) when EtOH was used[35]. If the goal were to synthesize compounds **7a** and **7b**, the method by Kim and co-workers would be a better method considering it uses less time, lower temperatures and produces higher yields.

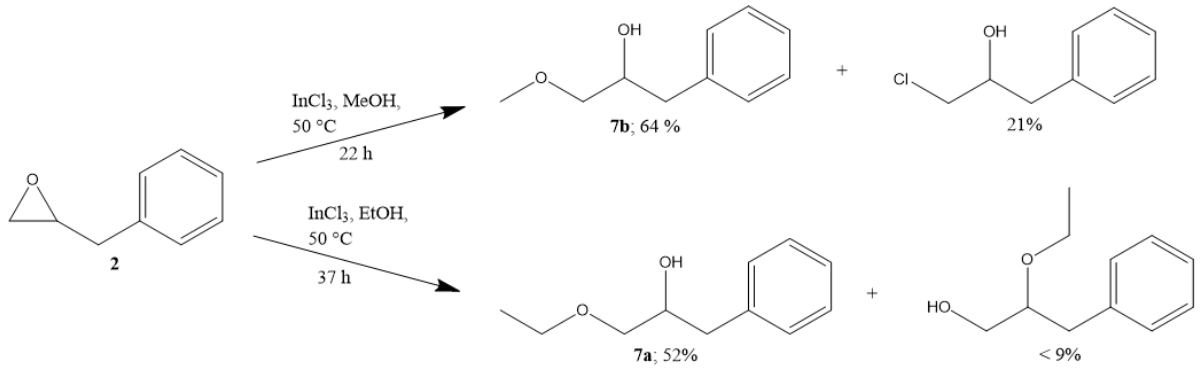

Scheme 8. Synthesis of compounds **7a** and **7b**, and 1-chloro-3-phenylpropan-2-ol and 2-ethoxy-3-phenylpropan-1-ol by Kim and co-workers[35].

2.2 Attempted syntheses of 1-((2,6-dichloro-4-nitrophenyl)amino)-3-phenylpropan-2-ol (**3b**) using LPDE and LPEtOAc

A Lewis-acid promoted epoxide ring opening method for reactions with poor nucleophiles was reported by Heydari and co-workers[21] and successfully used by Eikemo *et al*. for synthesizing ethanolamine derivatives[15,16,19]. This method uses 5 M LPDE and was used to attempt to synthesize compound **3b** (Scheme **9**).

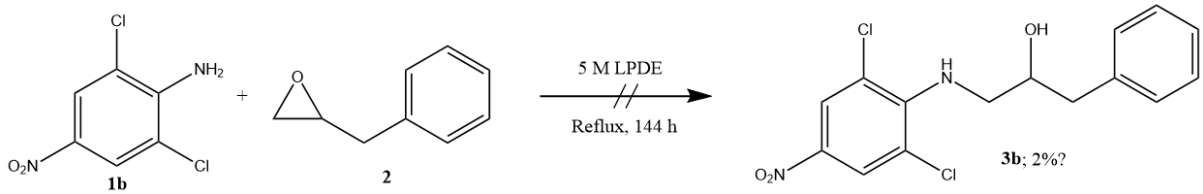

Scheme 9. Attempted synthesis of compound **3b** using 5 M LPDE.

The ^{1}H NMR spectra of the synthesis (Figure **4**) do have some peaks forming that could indicate formation of compound **3a**, however, these peaks are very small and only indicate 2% conversion according to the integrals of the peaks, with the rest of the crude being starting materials.

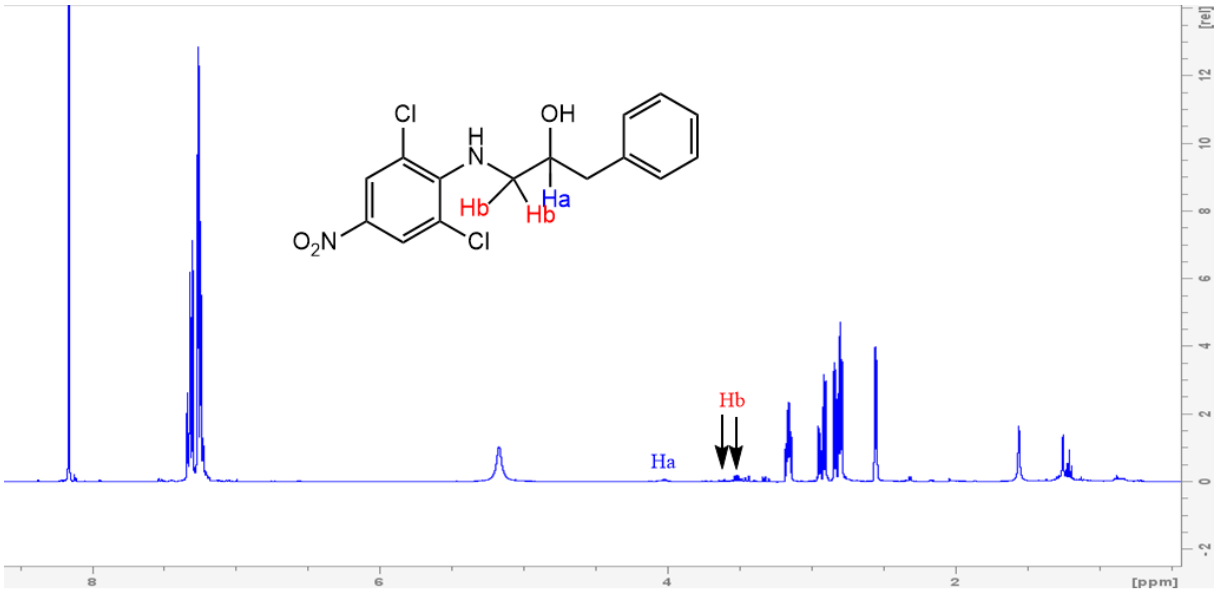

Figure 4. ^{1}H NMR spectra of crude product from reaction of compound **1b** and **2** in 5 M LPDE.

The poor reactivity of aniline **1b** can be explained by several reasons: Firstly, the compound would not dissolve properly in the reaction mixture. The law of mass action states that the rate of a chemical reaction is proportional to the product of the active masses of the reactants[34]. A solid reactant, such as aniline **1b**, has fewer active surfaces than a dissolved reactant, and therefore has a lower reaction rate than the reactant would have if fully dissolved. Secondly, aniline **1b** contains three EWG, which makes the aniline a poor nucleophile. In addition, the chlorides are in position 2 and position 6 on the aniline, and are large atoms with 35.45 g/mol per chloride atom compared to nitrogen with 14 g/mol and carbon with 12 g/mol. This results in steric hindrance, which further lowers the reaction rate. Compound **6k** synthesized by Eikemo *et al*. has a similar structure as compound **3b**, and gave a yield of 7%[16]. Although the yield of compound **6k** is low, it is higher than the conversion of compound **3b**, which can partly be explained by the size of the halogens. Fluorides are much smaller than chlorides, which results in less steric hindrance.

Eikemo *et al*. has previously used LPEtOAc instead of LPDE, and LPEtOAc was used in an attempt to synthesize compound **3b** (Scheme **10**).

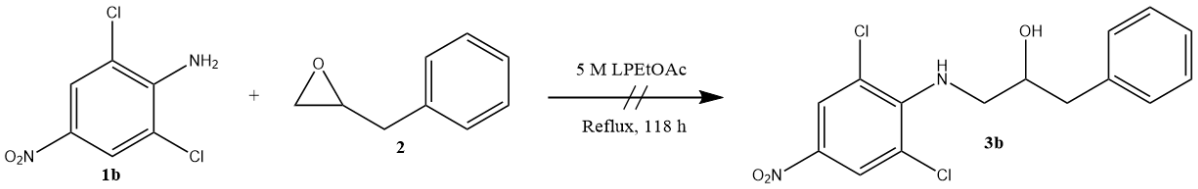

Scheme 10. Attempted synthesis of ethanolamine **3b** using 5 M LPEtOAc.

The reaction above resulted in an unknown side product instead of the intended target compound. This reaction was done twice to eliminate the chance of a human error, however, both reactions gave the same product as indicated by the ^{1}H NMR's (Figure **5**).

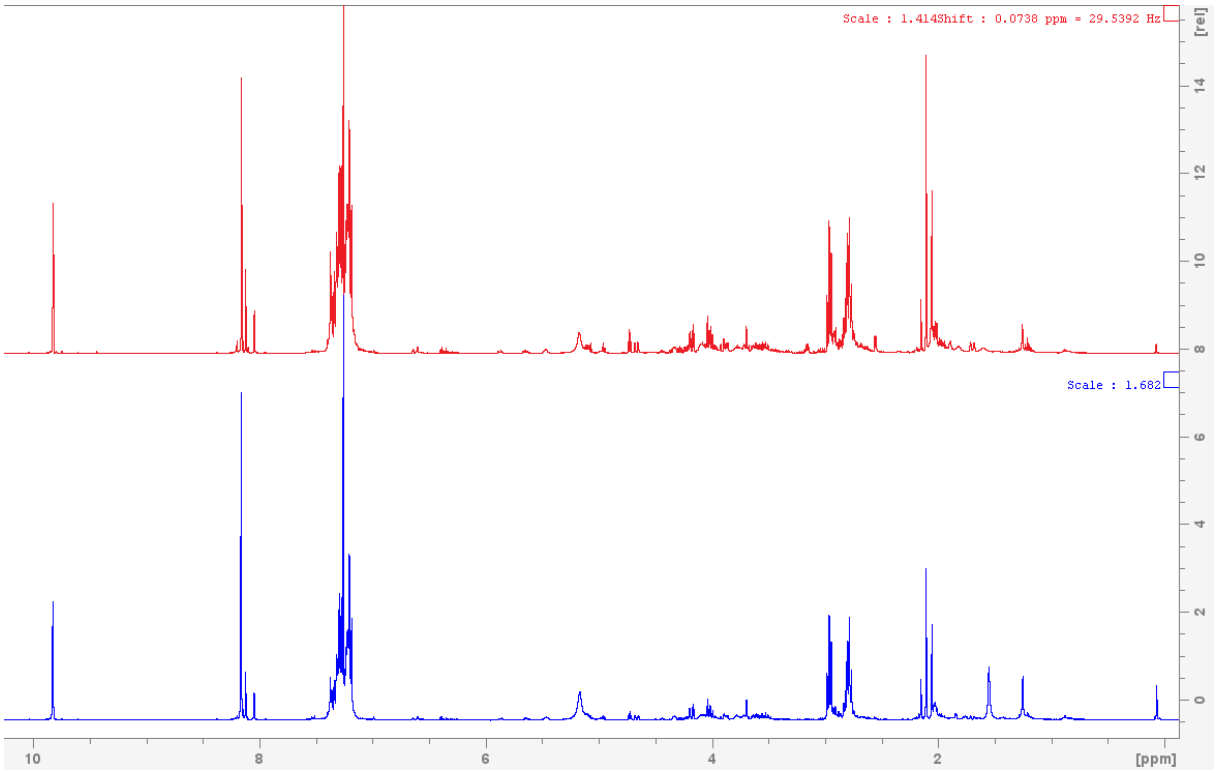

Figure 5. ^{1}H NMR spectra of crude products from attempted synthesis of compound **3b** in 5 M LPEtOAc.

One theory was that the crude product in Figure **5** consisted of 2-phenylacetaldehyde and 1-phenylpropan-2-one considering a similar product resulted from a reaction using 5 M LPEtOAc when Eikemo *et al*. was trying to determine the mechanism for photodegradation of ethanolamines[16,19]. The ^{1}H NMR specter, however, did not contain the peaks necessary to determine if this was the case, and further analyses would need to be done to determine the product of the reaction.

2.3 Syntheses of 1-((2,5-dichloro-4-nitrophenyl)amino)-3-phenylpropan-2-ol (**3a**) using LPDE and LPEtOAc

The synthesis of ethanolamine **3a** using 5 M LPDE was successful, although the compound was synthesized in a low yield of 12% (Scheme **11**). The conversion of the reaction in Scheme **11** was 17% according to the integrals of the relevant peaks in the reaction's crude ^{1}H NMR (Figure **6**), however, the low isolated yield of 12% is due to overlapping fractions.

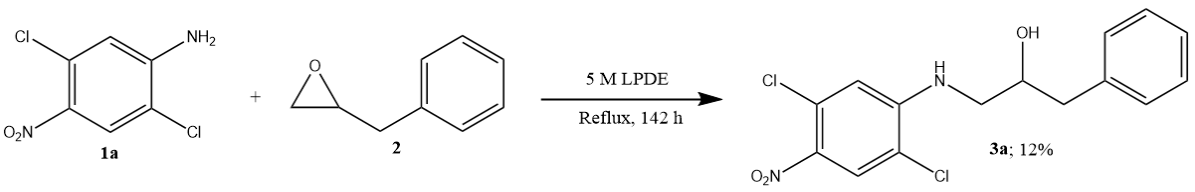

Scheme 11. Synthesis of ethanolamine **3a** using 5 M LPDE.

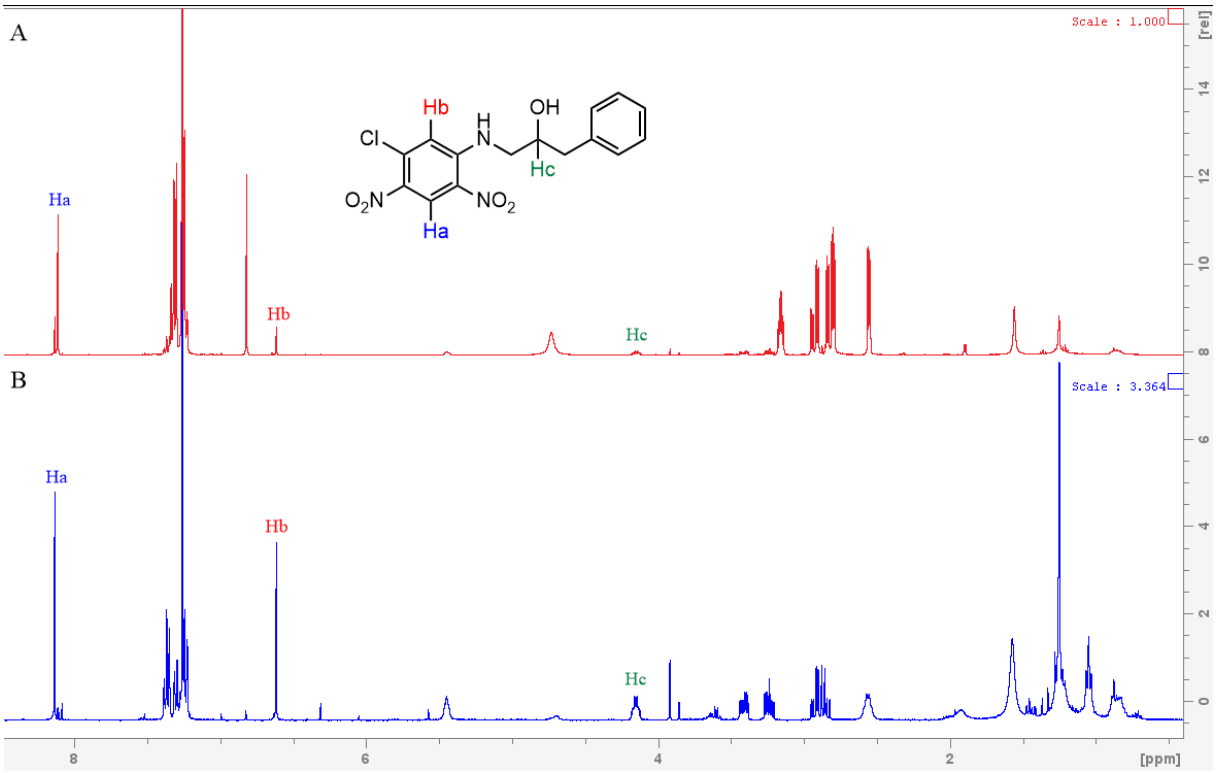

Figure 6. ^{1}H NMR spectra of (A) crude product and (B) isolated product from synthesis of compound **3a** in 5 M LPDE.

The reason for the low conversion of the reaction is again due to the poor nucleophilicity of aniline **1a**. Yet the conversion is much higher than when the same reaction conditions were employed with aniline **1b**, and this is due to the chloride in position 6 in aniline **1b** is instead in position 5 in aniline **1a**. This causes there to be significantly less steric hindrance in aniline **1a** compared to **1b**, which improves conversion and yield of ethanolamine **3a**.

Ethanolamine **3a** shares some similarities with compound **6f** synthesized by Eikemo *et al*. using the same reaction conditions. Both ethanolamines have a nitro-group in the *para*-position on the aniline and two chlorides on the aniline. Compound **6f** also contains a fluoride on the aniline and a chloride on the epoxide and was synthesized to a yield of 15%[16]. The extra EWG on the aniline makes it a poorer nucleophile, however, the electron-withdrawing chloride on the epoxide makes it a slightly better electrophile and it is therefore reasonable that the yield of compound **3a** is comparable to the yield of compound **6f**.

The same reaction, using compounds **1a** and **2**, was run in 5 M LPEtOAc to increase the yield of ethanolamine **3a** (Scheme **12**). The first attempt of this reaction resulted in a yield of 0% due to overlapping fractions, and a conversion of 71%. The reaction was run again and gave a yield of 13% and a conversion of 63%, again due to overlapping fractions. The first attempt was run for 91 h, while the second attempt was run for 147 h, yet it resulted in a lower conversion. At 72 h of the second attempt, it only had a conversion of 37% (Appendix, Figure **11**). This means that the reaction is not fully repeatable and running the reaction for a longer time does not

necessarily result in a higher conversion and yield. Nevertheless, this reaction is very promising and could result in good yields with better purification of the mixed fractions.

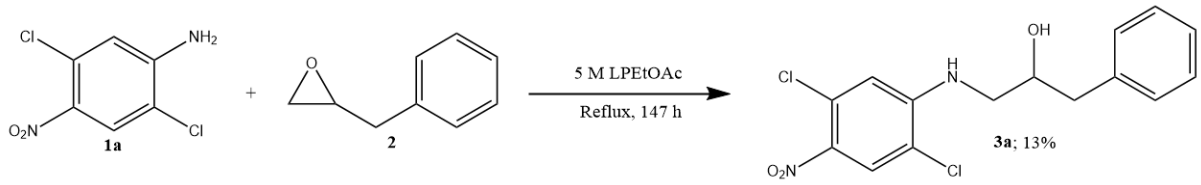

Scheme 12. Synthesis of ethanolamine **3a** using 5 M LPEtOAc.

Through examining the ^{1}H NMR spectra (Figure **7**) of the two attempts two synthesize ethanolamine **3a** and comparing the mixed fraction (Figure **7**, specter A) with the pure fraction (Figure **7**, specter B), several peaks can be seen in specter A that cannot be found in specter B. One peak that can be seen in specter A is overlapping with the peak for the hydrogen on the same carbon as the hydroxy-group (Hc). Further analyses would need to be done to determine what other chemical(s) are in the mixed fraction.

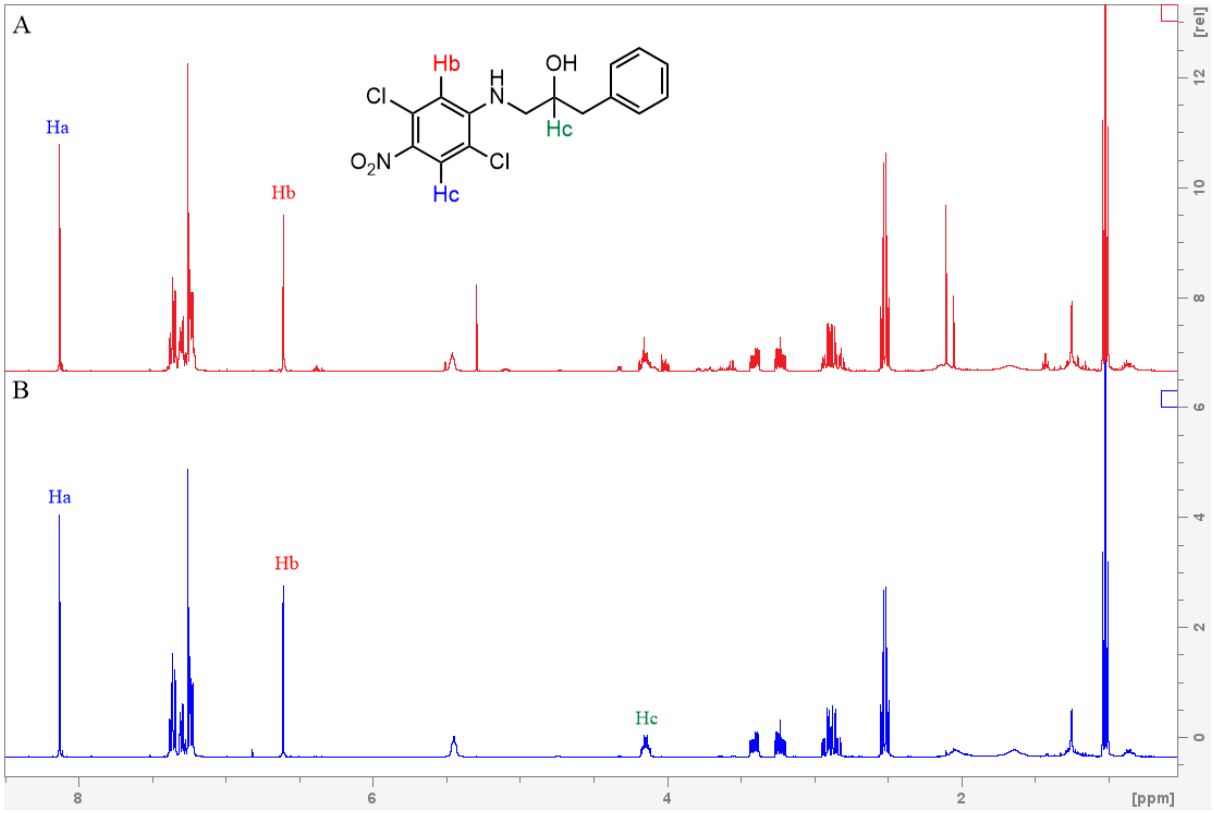

Figure 7. ^{1}H NMR spectra displaying (A) mixed fraction from first attempt to synthesize ethanolamine **3a** in 5 M LPEtOAc and (B) pure fraction of ethanolamine **3a** from the second attempt using 5 M LPEtOAc.

2.4 Synthesis of 5-benzyl-3-(2,5-dichloro-4-nitrophenyl)oxazolidine (**4**)

A fraction of compound **3a** with 86% purity as judged by ^{1}H NMR (Appendix, Figure **12**) was reacted with formaldehyde to give compound **4** to a yield of 31% (Scheme **13**). The ^{1}H NMR of the crude product showed a conversion of 43%, however all of compound **4** came out as one pure fraction in the purification process, which means some of the product was likely lost in the purification process.

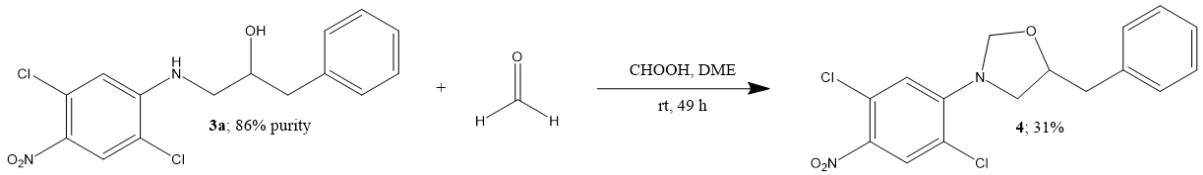

Scheme 13. Synthesis of compound **4** using ethanolamine **3a** and formaldehyde.

The formation of compound **4** is evident by the crude ^{1}H NMR (Figure **8**). This is due to the formation of two doublets that are not present on the ^{1}H NMR of ethanolamine **3a**. These two doublets are the hydrogens on the new carbon in the oxazolidine moiety, at 5.28 ppm and 5.20 ppm.

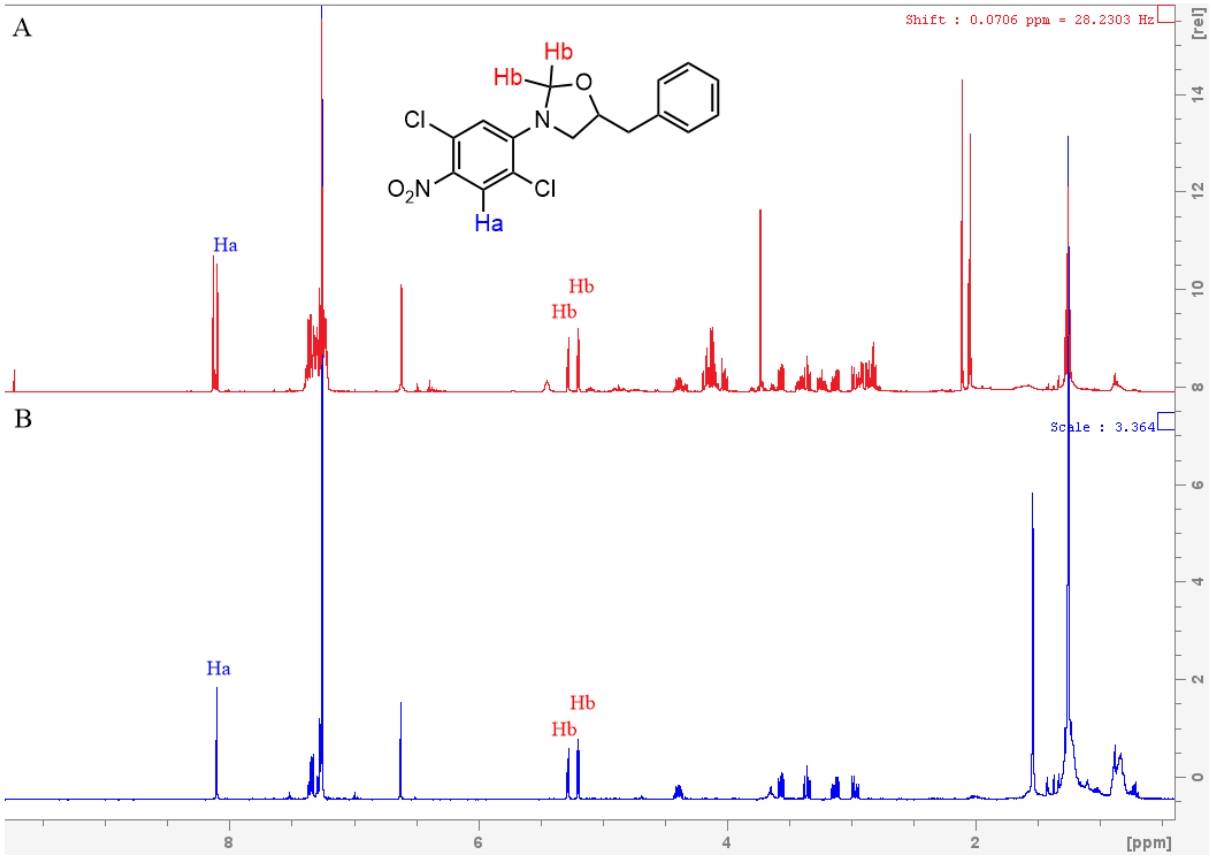

Figure 8. ^{1}H NMR of (A) crude product and (B) purified product from synthesis of compound **4**.

The product was synthesized in a decent yield (31%) using a non-pure fraction of the ethanolamine, however, the reaction should be performed again with a pure fraction, which could result in a better yield.

2.5 Photodecomposition studies

With two of the intended target compounds synthesized, ethanolamine **3a** and oxazolidine **4**, a photodecomposition could be conducted for the two compounds. The relevant aniline (**1a**) was also subjected to photodecomposition. Compounds **1a**, **3a** and **4** was analyzed by UV-vis spectroscopy to determine the λ_{max} and the molar attenuation coefficient, ε, for all the compounds (Figure **9**).

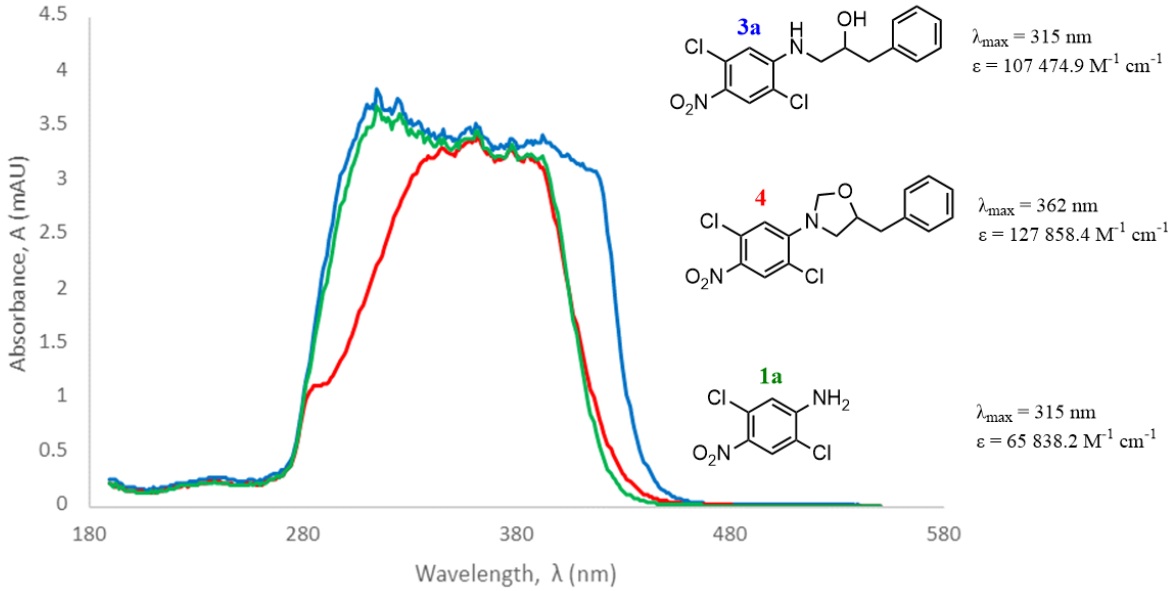

Figure 9. UV-vis spectra for compounds **1a**, **3a** and **4**. Concentrations were 2.3 mM for aniline **1a**, 1.17 mM for ethanolamine **3a**, and 1.13 mM for oxazolidine **4**. ε was calculated using Beer Lambert's Law; A = εcl.

The compounds were photolyzed in acetonitrile (ACN) and water (7:3) at pH = 7, following the procedure by Wan and Muralidharan[17] and used by Eikemo *et al.*[15,16,19]. A 125 W medium-pressure mercury lamp was used, with strong emissions above 300 nm, and the solutions containing the relevant compound were irradiated for approximately 24 h. The products were extracted with EtOAc, followed by analysis with ^{1}H NMR spectroscopy (Figure **10**).

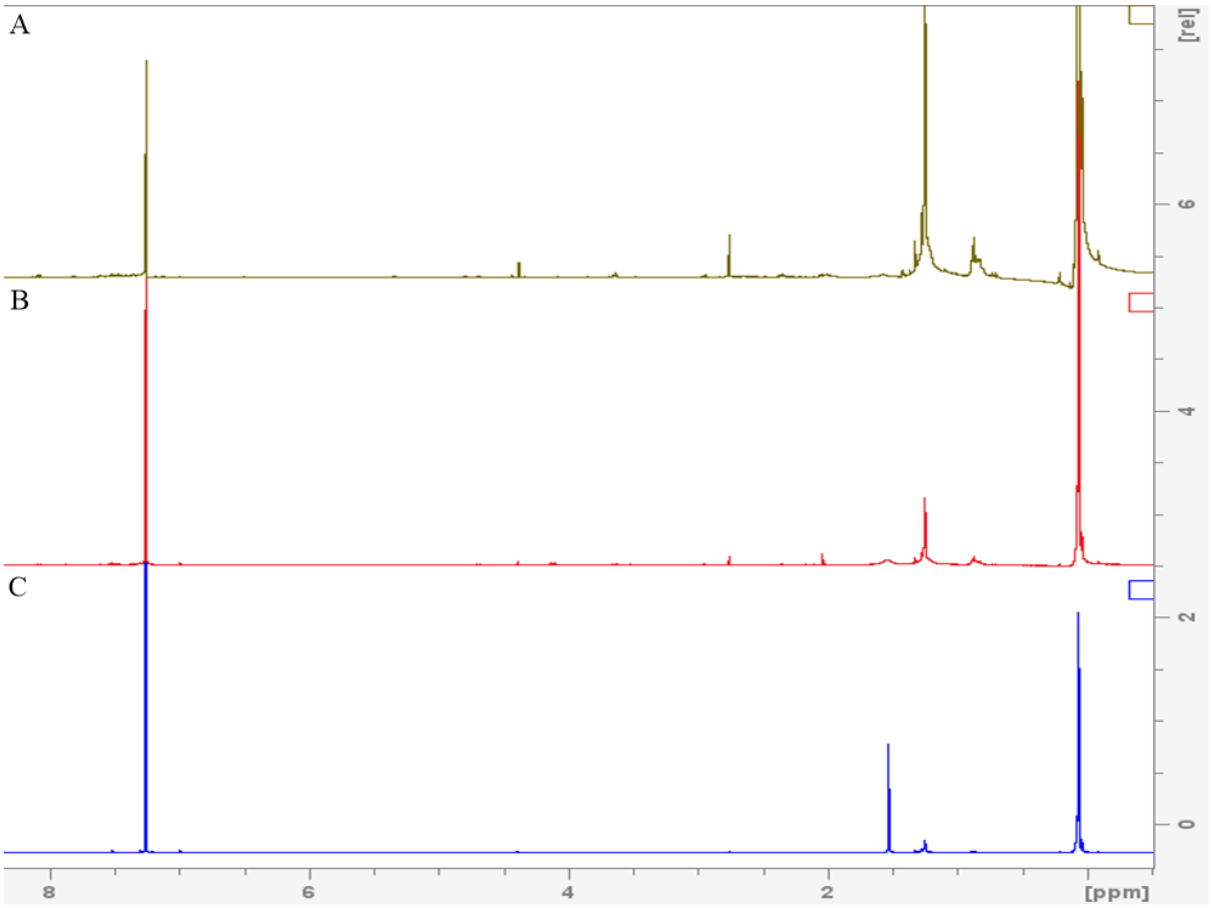

Figure 10. ^{1}H NMR of the photodecomposition products of (A) ethanolamine **3a**, (B) oxazolidine **4** and (C) aniline **1a**.

It is evident by the ^{1}H NMR spectra in Figure **10** that compounds **1a**, **3a** and **4** decomposed fully when irradiated by UV-light for ~24 hours. None of the spectra contains a peak at 10.02 ppm that would indicate formation of benzaldehyde, which suggests that the photodecompositions of these compounds does not follow the same decomposition mechanism that was elucidated by Eikemo *et al.*[16,19]. While most of the peaks are due to residual solvents and water[36], there is one peak at 4.38 ppm and one peak at 2.77 ppm that are visible in spectra A and B that could be hydrogens in the photodecomposition products. However, the spectra do not contain enough peaks to account for all the hydrogens in the starting materials, which indicates that part of the decomposition products were lost in the work-up due to being dissolved in the aquatic phase. It is also worth noting that aniline **1a** also fully decomposed, as the peaks at 8.12 ppm and 6.83 ppm (Appendix, Figure **13**) are fully gone. Aniline **1a** is chronically toxic to aquatic life[37], so the photodecomposition of the aniline is very promising as it could result in less toxicity. Further analyses of the decomposition products need to be done to elucidate the decomposition mechanisms of compounds **1a**, **3a** and **4**.

2.6 Summary of results

Table **1** shows a summary of all reactions with the crude conversion and yield given for each reaction. The synthesis of ethanolamine **3a** in 5 M LPDE resulted in a yield of 12%. The synthesis of ethanolamine **3a** in 5 M LPEtOAc resulted in the best yield of 13%, with a much higher conversion of 63%. As previously discussed, this is due to overlapping fractions. All the photodecompositions that were performed resulted in 100% decomposition of the relevant compound. None of the other reactions worked as intended.

Reaction	Crude conversion (%)	Yield (%)
Synthesis of **7a** using **1a**	23	-
Synthesis of **7a** using **1b**	13	-
Synthesis of **7b**	47	-
Synthesis of **7c**	66	-
Synthesis of **3b** using 5 M LPDE	≤ 2	-
Synthesis of **3b** using 5 M LPEtOAc	-	-
Synthesis of **3a** using 5 M LPDE	17	12
Synthesis of **3a** using 5 M LPEtOAc, attempt 1	71	0
Synthesis of **3a** using 5 M LPEtOAc, attempt 2	63	13
Synthesis of **4**	43	31
Photodecomposition of **3a**	100*	-
Photodecomposition of **4**	100*	-
Photodecomposition of **1a**	100*	-

Table 1. Summary of the results of all reactions, with the conversion and yield of each reaction. *Percentage of compound fully decomposed.

2.7 Further research

Ethanolamine **3b** was not successfully synthesized for the duration of this project. As previously discussed, there are certain similarities between compound **6k** synthesized by Eikemo *et al*. and ethanolamine **3b**. Eikemo *et al*. managed to successfully synthesize compound **6k** in very good yield (80%) using an alternative method (Scheme **14**). This method is based on the reversal role of the nucleophile and the electrophile and uses a ring opening of the epoxide with sodium azide followed by a Staudinger reduction. The synthesized 1,2-aminoalcohol can then readily react with the relevant nitrobenzene[16]. These reactions could possibly be used to synthesize ethanolamine **3b**, using compound **2** as the starting material and a nitrobenzene with chlorides in position 1 and 3 instead of fluorides.

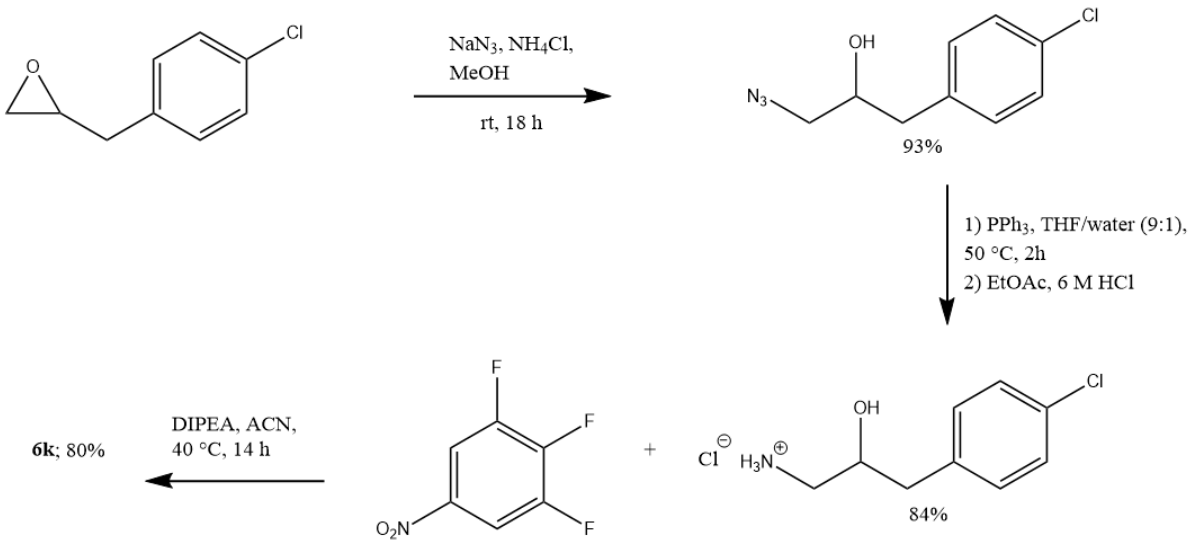

Scheme 14. Formation of ethanolamine **6k** by Eikemo *et al*. using an alternative method[16].

3 Concluding remarks

Ethanolamine **3a** was successfully synthesized to a yield of 13% in 5 M LPEtOAc. The crude conversion of the compound was 63%, and this difference between the yield and the conversion is due to overlapping fractions resulting from the purification process. The compound was also synthesized in 5 M LPDE, however, the reaction only produced a yield of 12% and a conversion of 17%. The synthesis using 5 M LPEtOAc proved to be the most promising reaction for synthesizing ethanolamine **3a**.

Several attempts were made to synthesize ethanolamine **3b**: In LiBr and various alcohols, which resulted in an epoxide ring opening the alcohol. Synthesis was also attempted using 5 M LPDE, which was not successful, and in 5 M LPEtOAc, which resulted in an unknown side product. An alternative method that was used by Eikemo *et al*. to synthesize ethanolamine **6k**[16] was suggested as a possible method for synthesizing ethanolamine **3a**.

Oxazolidine **4** was successfully synthesized to a yield of 31% and a conversion of 43%. A fraction of ethanolamine **3a** with 86% purity as judged by ^{1}H NMR was used to synthesize compound **4**. This reaction should be attempted again with a pure fraction, as this might result in a higher yield.

Compounds **1a**, **3a** and **4** were fully decomposed when irradiated by a 125 W medium-pressure mercury lamp in a solution of ACN and water (7:3) at a pH of 7 for approximately 24 hours. The decomposition products are unknown, and the decompositions do not follow the same mechanism that was elucidated by Eikemo *et al*. according to the ^{1}H NMR's. Further research should be done to determine the decomposition products and the decomposition mechanisms. The decomposition of aniline **1a** is very promising, as the compound is toxic to aquatic life[37].

4 Experimental section

4.1 General information

All chemicals were purchased from Sigma-Aldrich/Merck or VWR and used as supplied. When dry solvents were needed, they were dried by storing over 4 Å molecular sieves.

Thin layer chromatography (TLC) was done with silica gel (60 F_{254}) on aluminum sheets. A solvent system with various mixtures of petroleum ether, ethyl acetate and dichloromethane were used as the mobile phase. Visualization was achieved by UV light (254 nm) and/or a phosphomolybdic acid solution stain and heat.

Flash chromatography was done with a hand pump, 230-400 mesh silica gel and a solvent gradient based on the R_f value for the crude product by TLC.

NMR analyses were conducted on a Bruker Ascend 400 spectrometer operating at 400.13 MHz for ^{1}H and 100.61 MHz for ^{13}C. Coupling constants (J) are given in Hz, and the multiplicity is reported as singlet (s), doublet (d), triplet (t), quartet (q), sextet (sxt), multiplet (m), and broad singlet (bs). Chemical shifts are given in ppm, going from downfield to upfield, and calibration is done using the residual solvent signal for chloroform-d_3 (^{1}H 7.26 ppm; ^{13}C 77.16 ppm)[36].

UV-vis spectra were produced by a GENESYS 50 dual beam UV-vis spectrophotometer. The spectrophotometer uses dual silicon photodiode detectors. Samples were analyzed in an open-top UV quartz cell (10 mm, 2.0 mL) with ethanol as the solvent. Wavelengths are reported in nm, and the molar attenuation coefficients in M^{-1} cm^{-1}.

4.2 Synthesis procedures

*Synthesis of 1-((2,5-dichloro-4-nitrophenyl)amino)-3-phenylpropan-2-ol (**3a**) using EtOAc as solvent:*

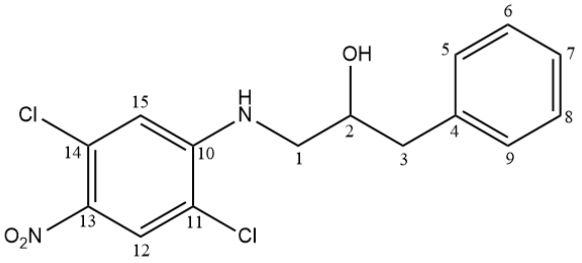

A dry round-bottom flask was charged with anhydrous $LiClO_4$ (5085 mg, 47.8 mmol) and dry EtOAc (9.6 mL) under argon and stirred until a homogenous solution. 2,5-dichloro-4-nitroaniline (**1a**) (200 mg, 0.956 mmol) and (2,3-epoxypropyl)benzene (**2**) (0.126 mL, 0.956 mmol) were added and the reaction mixture was hea1 ted at reflux for 147 h. The reaction was quenched with water (5 mL) and the crude product was extracted with EtOAc (3 x 10 mL). The organic layers were combined and washed with brine (10 mL). The crude product was dried ($MgSO_4$), filtered and concentrated in vacuo. . The crude product was evaporated on to celite

and applied to a prepacked column (the column was packed with pet. ether and 3% Et_3N). Column chromatography (pet. ether/DCM, 45:55 → 30:70) was followed by isolation of the relevant fractions (R_f = 0.53 in DCM), which gave 1-((2,5-dichloro-4-nitrophenyl)amino)-3-phenylpropan-2-ol (42.2 mg, 13%) as a yellow oil. UV-vis: λ_{max} (EtOH) 315 nm (ε 107,474.9 M^{-1} cm^{-1}); ^1H NMR (400 MHz, $CDCl_3$): δ 8.13 (s, 1H, H on C12), 7.40-7.20 (m, 5H, H on C5-C9), 6.61 (s, 1H, H on C15), 5.45 (bs, 1H, H in OH-group), 4.19-4.11 (m, 1H, H on C2), 3.41 (dd, *J* = 2 Hz, 13 Hz, 1H, H on C1), 3.24 (dd, *J* = 5 Hz, 13 Hz, 1H, H on C1), 2.89 (dd, *J* = 5 Hz, 14 Hz, 2H, H on C3); ^{13}C NMR (100 MHz, $CDCl_3$): δ 148.1 (C10), 136.7 (C4), 135.8 (C13), 129.6 (C14), 129.4 (C5 and C9), 129.2 (C6 and C8), 127.9 (C12), 127.4 (C7), 117.0 (C11), 112.1 (C15), 71.0 (C2), 48.2 (C1), 41.9 (C3). Sample for HRMS will be sent for analysis.

*Synthesis of 1-((2,5-dichloro-4-nitrophenyl)amino)-3-phenylpropan-2-ol (**3a**) using Et_2O as solvent:*

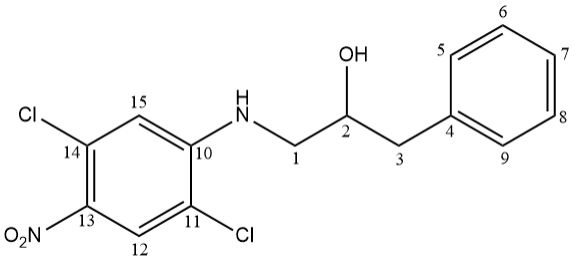

A dry round-bottom flask was charged with anhydrous $LiClO_4$ (2660 mg, 0.239 mmol) and dry Et_2O (5 mL) under argon. The reaction mixture was stirred and sonicated until a homogenous LPDE-solution. The round-bottom flask was charged with 2,5-dichloro-4-nitroaniline (**1a**) (100 mg, 0.478 mmol) and (2,3-epoxypropyl)benzene (**2**) (0.063 mL, 0.478 mmol), and heated at reflux for 142 h under argon. The reaction was quenched with water (5 mL) and the crude product was extracted with EtOAc (3 x 10 mL). The organic layers were combined and washed with brine (10 mL). The crude product was dried ($MgSO_4$), filtered and concentrated in vacuo. The crude product was evaporated on to celite and applied to a prepacked column (the column was packed with pet. ether and 3% Et_3N). Column chromatography (pet. ether/DCM, 3:7 → 2:8) was followed by isolation of the relevant fractions (R_f = 0.22 in pet. ether/DCM, 1:9), which gave 1-((2,5-dichloro-4-nitrophenyl)amino)-3-phenylpropan-2-ol (20.0 mg, 12%) as a yellow oil. Spectroscopic data is in accordance with data reported of the previous synthesis.

*Synthesis of 5-benzyl-3-(2,5-dichloro-4-nitrophenyl)oxazolidine (**4**):*

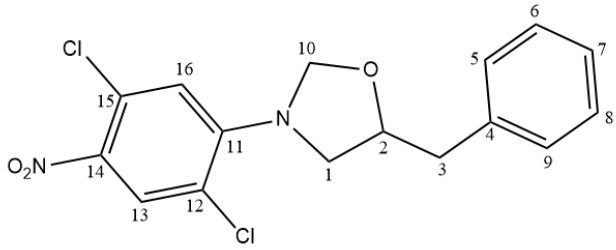

1-((2,5-dichloro-4-nitrophenyl)amino)-3-phenylpropan-2-ol (**3a**) (134 mg, 0.34 mmol) with 86% purity as judged by ^1H NMR was dissolved in DCE (7.85 mL) in a round-bottom flask

under argon. 37% formaldehyde (0.135 mL, 1.73 mmol) and formic acid (0.016 mL, 0.43 mmol) were added, and the reaction mixture was stirred at rt for 49 h. The reaction was quenched with water (5 mL) and the crude product was extracted with EtOAc (3 x 10 mL). The organic layers were combined and washed with brine (10 mL). The crude product was dried ($MgSO_4$), filtered and concentrated in vacuo. The crude was evaporated on to celite and applied to a prepacked column (the column was packed with pet. ether and 3% Et_3N). Column chromatography (pet. ether/EtOAc, 95:5 → 40:60) was followed by isolation of the relevant fractions (R_f = 0.70 in pet. ether/EtOAc, 4:6) which gave 5-benzyl-3-(2,5-dichloro-4-nitrophenyl)oxazolidine (36.9 mg, 31%) as a dark yellow oil. UV-vis: λ_{max} (EtOH) 362 nm (ε 127,858.4 M^{-1} cm^{-1}); ^{1}H NMR (400 MHz, $CDCl_3$): δ 8.10 (s, 1H, H on C13), 7.38-7.27 (m, 5H, H on C5-C9), 6.63 (s, 1H, H on C16), 5.28 (d, *J* = 4 Hz, 1H, H on C10), 5.20 (d, *J* = 4 Hz, 1H, H on C10), 4.43-4.35 (m, 1H, H on C2), 3.57 (dd, *J* = 6 Hz, 9 Hz, 1H, H on C1), 3.36 (dd, *J* = 9 Hz, 1H, H on C1), 3.13 (dd, *J* = 7 Hz, 14 Hz, 1H, H on C3), 2.97 (dd, *J* = 6 Hz, 14 Hz, 1H, H on C3). Sample for HRMS will be sent for analysis.

*Attempted synthesis of 1-((2,5-dichloro-4-nitrophenyl)amino)-3-phenylpropan-2-ol (**3a**) with formation of 1-ethoxy-3-phenylpropan-2-ol (**7a**):*

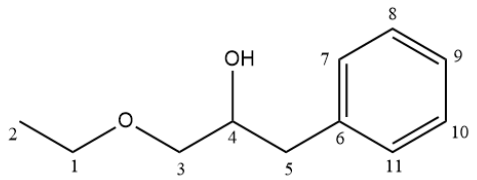

LiBr (41.5 mg, 0.478 mmol) was dissolved in EtOH (1.6 mL) in a vial. 2,5-dichloro-4-nitroaniline (**1a**) (200 mg, 0.957 mmol) and (2,3-epoxypropyl)benzene (**2**) (0.126 mL, 0.957 mmol) were added, and the reaction mixture was heated for 119 h. The reaction was quenched with water (5 mL) and the crude product was extracted with EtOAc (3 x 10 mL). The organic layers were combined and washed with brine (10 mL). The crude product was dried ($MgSO_4$), filtered and concentrated in vacuo. The work-up gave a crude product with 1-ethoxy-3-phenylpropan-2-ol (**7a**) (426 mg, 23% conversion). No purification or isolation was done on the crude. R_f = 0.06 in pet. ether/DCM, 3:7 (for 1-ethoxy-3-phenylpropan-2-ol). ^{1}H NMR (400 MHz, $CDCl_3$): δ 7.35-7.20 (m, 5H, H on C7-C11), 4.73 (bs, 1H, H in OH-group), 4.06-3.99 (m, 1H, H on C4), 3.57-3.48 (m, 2H, H on C1), 3.45 (dd, *J* = 4 Hz, 10 Hz, 1H, H on C3), 3.32 (dd, J = 7 Hz, 10 Hz, 1H, H on C3), 2.84 (d, *J* = 5 Hz, 1H, H on C5), 2.32 (d, *J* = 4 Hz, 1H, H on C5), 1.21 (t, *J* = 7 Hz, 3H, H on C2). Spectroscopic data are in accordance with previously reported data[35].

*Attempted synthesis of 1-((2,6-dichloro-4-nitrophenyl)amino)-3-phenylpropan-2-ol (**3b**) with formation of 1-ethoxy-3-phenylpropan-2-ol (**7a**)*:

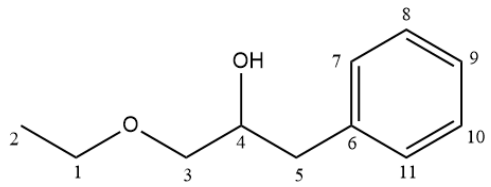

LiBr (20.8 mg, 0.239 mmol) was dissolved in EtOH (2.4 mL) in a vial. 2,6-dichloro-4-nitroaniline (**1b**) (100 mg, 0.478 mmol) and (2,3-epoxypropyl)benzene (**2**) (0.063 mL, 0.478 mmol) were added, and the reaction mixture was heated for 117 h. The reaction was quenched with water (5 mL) and the crude product was extracted with EtOAc (3 x 10 mL). The organic layers were combined and washed with brine (10 mL). The crude product was dried ($MgSO_4$), filtered and concentrated in vacuo. The work-up gave a crude product with 1-ethoxy-3-phenylpropan-2-ol (**7a**) (255.1 mg, 13% conversion). No purification or isolation was done on the crude. R_f = 0.11 in pet. ether/DCM, 3:7 (for 1-ethoxy-3-phenylpropan-2-ol). Spectroscopic data is in accordance with data reported of the previous synthesis and previously reported data[35].

*Attempted synthesis of 1-((2,5-dichloro-4-nitrophenyl)amino)-3-phenylpropan-2-ol (**3a**) with formation of 1-methoxy-3-phenylpropan-2-ol (**7b**)*:

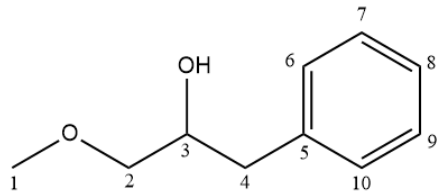

LiBr (20.8 mg, 0.239 mmol) was dissolved in MeOH (0.8 mL) in a vial. 2,5-dichloro-4-nitroaniline (**1a**) (100 mg, 0.478 mmol) and (2,3-epoxypropyl)benzene (**2**) (0.063 mL, 0.478 mmol) were added, and the reaction mixture was heated for 73 h. The reaction was quenched with water (5 mL) and the crude product was extracted with EtOAc (3 x 10 mL). The organic layers were combined and washed with brine (10 mL). The crude product was dried ($MgSO_4$), filtered and concentrated in vacuo. The crude was evaporated on to celite and applied to a prepacked column (the column was packed with DCM and 3% Et_3N). Column chromatography (DCM/EtOAc, 10:0 → 8:2) was followed by isolation of the relevant fractions (R_f = 0.71 in DCM/EtOAc, 8:2) which gave 1-methoxy-3-phenylpropan-2-ol (**7b**) (0 mg, 0%) in mixed fractions. ^{1}H NMR (400 MHz, $CDCl_3$): δ 7.39-7.21 (m, 5H, H on C6-C10), 4.73 (bs, 1H, H in OH-group), 4.06-3.98 (m, 1H, H on C3), 3.42 (dd, J = 4 Hz, 10 Hz, 1H, H on C2), 3.39 (s, 3H, H on C1), 3.30 (dd, J = 7 Hz, 10 Hz, 1H, H on C2), 2.80 (dd, J = 3 Hz, 7 Hz, 2H, H on C4). Spectroscopic data are in accordance with previously reported data[35].

*Attempted synthesis of 1-((2,5-dichloro-4-nitrophenyl)amino)-3-phenylpropan-2-ol (**3a**) with formation of 1-phenyl-3-(2,2,2-trifluoroethoxy)propan-2-ol (**7c**):*

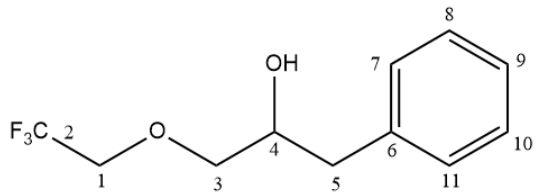

LiBr (20.8 mg, 0.239 mmol) was dissolved in CF_3CH_2OH (0.8 mL) in a vial. 2,5-dichloro-4-nitroaniline (**1a**) (100 mg, 0.478 mmol) and (2,3-epoxypropyl)benzene (**2**) (0.063 mL, 0.478 mmol) were added, and the reaction mixture was heated for 119 h. The reaction was quenched with water (5 mL) and the crude product was extracted with EtOAc (3 x 10 mL). The organic layers were combined and washed with brine (10 mL). The crude product was dried ($MgSO_4$), filtered and concentrated in vacuo. The work-up gave a crude product with 1-phenyl-3-(2,2,2-trifluoroethoxy)propan-2-ol (**7c**) (330.7 mg, 66% conversion) as a light-yellow powder. No purification or isolation was done on the crude. R_f = 0.06 in pet. ether/DCM, 3:7 (for 1-ethoxy-3-phenylpropan-2-ol). ^{1}H NMR (400 MHz, $CDCl_3$): δ 7.37-7.19 (m, 5H, H on C7-C11), 4.73 (bs, 1H, H in OH-group), 4.09-4.01 (m, 1H, H on C4), 3.88 (q, *J* = 8 Hz, 17 Hz, 2H, H on C1), 3.67 (dd, *J* = 10 Hz, 13 Hz, 1H, H on C3), 3.54 (dd, *J* = 7 Hz, 10 Hz, 1H, H on C3), 2.82 (d, *J* = 6 Hz, 2H, H on C5).

General procedure for photodecomposition: A 125 W medium-pressure mercury lamp is used for $\lambda_{max} > 300$ nm. The appropriate compound (30-50 mg) was dissolved in ACN (52.5 mL) and added to a photochemical Pyrex reactor containing distilled water at pH = 7 (22.5 mL) (ACN/water, 7:3. The reaction mixture was photolyzed with the 125 W medium-pressure mercury lamp for approximately 24 h.

*Photolysis of 1-((2,5-dichloro-4-nitrophenyl)amino)-3-phenylpropan-2-ol (**3a**):* A solution of 1-((2,5-dichloro-4-nitrophenyl)amino)-3-phenylpropan-2-ol (**3a**) (30 mg, 0.088 mmol) was photolyzed in a 75 mL (1.17 mM) photochemical reactor according to the general procedure for 25 h. ACN was evaporated off on a rotavapor, and an extraction was done with EtOAc (3 x 10 mL), and the organic layers were combined and washed with brine (10 mL). The crude product was dried ($MgSO_4$), filtered and concentrated in vacuo and analyzed by ^{1}H NMR.

*Photolysis of 5-benzyl-3-(2,5-dichloro-4-nitrophenyl)oxazolidine (**4**):* A solution of 5-benzyl-3-(2,5-dichloro-4-nitrophenyl)oxazolidine (**4**) (30 mg, 0.085 mmol) was photolyzed in a 75 mL (1.13 mM) photochemical reactor according to the general procedure for 21 h. ACN was evaporated off on a rotavapor, and an extraction was done with EtOAc (3 x 10 mL), and the organic layers were combined and washed with brine (10 mL). The crude product was dried ($MgSO_4$), filtered and concentrated in vacuo and analyzed by ^{1}H NMR.

*Photolysis of 2,5-dichloro-4-nitroaniline (**1a**):* UV-vis: λ_{max} (EtOH) 315 nm (ε 65,838.2 M^{-1} cm^{-1}). A solution of 2,5-dichloro-4-nitroaniline (**1a**) (35 mg, 0.17 mmol) was photolyzed in a 75 mL (2.3 mM) photochemical reactor according to the general procedure for 24 h. ACN was

evaporated off on a rotavapor, and an extraction was done with EtOAc (3 x 10 mL), and the organic layers were combined and washed with brine (10 mL). The crude product was dried ($MgSO_4$), filtered and concentrated in vacuo and analyzed by ^1H NMR.

5 References

(1) Sherma, J.; Choma, I. In *Handbook of Thin-Layer Chromatography*; CRC Press, 2003; Vol. 89, pp 1–2 and 543–545.

(2) Fleming, A. On the Antibacterial Action of Cultures of a Penicillium, with Special Reference to Their Use in the Isolation of B. Influenzæ. *Br. J. Exp. Pathol.* **1929**, *10*, 226–236.

(3) Ventola, L. C. The Antibiotic Resistance Crisis. *Pharmacy and Therapeutics* **2015**, *40*, 277–283.

(4) Fischbach, M. A.; Walsh, C. T. Antibiotics for Emerging Pathogens. *Science* **2009**, *325*, 1089–1093.

(5) Murray, C. J. L.; Ikuta, K. S.; Sharara, F.; Swetschinski, L.; Robles Aguilar, G.; Gray, A.; Han, C.; Bisignano, C.; Rao, P.; Wool, E.; Johnson, S. C.; Browne, A. J.; Chipeta, M. G.; Fell, F.; Hackett, S.; Haines-Woodhouse, G.; Kashef Hamadani, B. H.; Kumaran, E. A. P.; McManigal, B.; Achalapong, S.; Agarwal, R.; Akech, S.; Albertson, S.; Amuasi, J.; Andrews, J.; Aravkin, A.; Ashley, E.; Babin, F.-X.; Bailey, F.; Baker, S.; Basnyat, B.; Bekker, A.; Bender, R.; Berkley, J. A.; Bethou, A.; Bielicki, J.; Boonkasidecha, S.; Bukosia, J.; Carvalheiro, C.; Castañeda-Orjuela, C.; Chansamouth, V.; Chaurasia, S.; Chiurchiù, S.; Chowdhury, F.; Clotaire Donatien, R.; Cook, A. J.; Cooper, B.; Cressey, T. R.; Criollo-Mora, E.; Cunningham, M.; Darboe, S.; Day, N. P. J.; De Luca, M.; Dokova, K.; Dramowski, A.; Dunachie, S. J.; Duong Bich, T.; Eckmanns, T.; Eibach, D.; Emami, A.; Feasey, N.; Fisher-Pearson, N.; Forrest, K.; Garcia, C.; Garrett, D.; Gastmeier, P.; Giref, A. Z.; Greer, R. C.; Gupta, V.; Haller, S.; Haselbeck, A.; Hay, S. I.; Holm, M.; Hopkins, S.; Hsia, Y.; Iregbu, K. C.; Jacobs, J.; Jarovsky, D.; Javanmardi, F.; Jenney, A. W. J.; Khorana, M.; Khusuwan, S.; Kissoon, N.; Kobeissi, E.; Kostyanev, T.; Krapp, F.; Krumkamp, R.; Kumar, A.; Kyu, H. H.; Lim, C.; Lim, K.; Limmathurotsakul, D.; Loftus, M. J.; Lunn, M.; Ma, J.; Manoharan, A.; Marks, F.; May, J.; Mayxay, M.; Mturi, N.; Munera-Huertas, T.; Musicha, P.; Musila, L. A.; Mussi-Pinhata, M. M.; Naidu, R. N.; Nakamura, T.; Nanavati, R.; Nangia, S.; Newton, P.; Ngoun, C.; Novotney, A.; Nwakanma, D.; Obiero, C. W.; Ochoa, T. J.; Olivas-Martinez, A.; Olliaro, P.; Ooko, E.; Ortiz-Brizuela, E.; Ounchanum, P.; Pak, G. D.; Paredes, J. L.; Peleg, A. Y.; Perrone, C.; Phe, T.; Phommasone, K.; Plakkal, N.; Ponce-de-Leon, A.; Raad, M.; Ramdin, T.; Rattanavong, S.; Riddell, A.; Roberts, T.; Robotham, J. V.; Roca, A.; Rosenthal, V. D.; Rudd, K. E.; Russell, N.; Sader, H. S.; Saengchan, W.; Schnall, J.; Scott, J. A. G.; Seekaew, S.; Sharland, M.; Shivamallappa, M.; Sifuentes-Osornio, J.; Simpson, A. J.; Steenkeste, N.; Stewardson, A. J.; Stoeva, T.; Tasak, N.; Thaiprakong, A.; Thwaites, G.; Tigoi, C.; Turner, C.; Turner, P.; van Doorn, H. R.; Velaphi, S.; Vongpradith, A.; Vongsouvath, M.; Vu, H.; Walsh, T.; Walson, J. L.; Waner, S.; Wangrangsimakul, T.; Wannapinij, P.; Wozniak, T.; Young Sharma, T. E. M. W.; Yu, K. C.; Zheng, P.; Sartorius, B.; Lopez, A. D.; Stergachis, A.; Moore, C.; Dolecek, C.; Naghavi, M. Global Burden of Bacterial Antimicrobial Resistance in 2019: A Systematic Analysis. *The Lancet* **2022**, *399*, 629–655.

(6) Kümmerer, K. Resistance in the Environment. *J. Antimicrob. Chemother.* **2004**, *54*, 311–320.

(7) Van Boeckel, T. P.; Pires, J.; Silvester, R.; Zhao, C.; Song, J.; Criscuolo, N. G.; Gilbert, M.; Bonhoeffer, S.; Laxminarayan, R. Global Trends in Antimicrobial Resistance in Animals in Low- and Middle-Income Countries. *Science* **2019**, *365*, eaaw1944.

(8) Hanna, N.; Tamhankar, A. J.; Lundborg, C. S. Antibiotic Concentrations and Antibiotic Resistance in Aquatic Environments of the WHO Western Pacific and South-East Asia

Regions: A Systematic Review and Probabilistic Environmental Hazard Assessment. *Lancet* **2023**, *7*, e45-54.
(9) Gartiser, S.; Urich, E.; Alexy, R.; Kümmerer, K. Ultimate Biodegradation and Elimination of Antibiotics in Inherent Tests. *Chemosphere* **2006**, *67*, 604–613.
(10) Sydnes, M. O. Drugs Designed for Degradation in the Environment Post Use. *Curr. Green Chem.* **2023**, *10*, 92–97.
(11) Kümmerer, K. Sustainable from the Very Beginning: Rational Design of Molecules by Life Cycle Engineering as an Important Approach for Green Pharmacy and Green Chemistry. *Green Chem.* **2007**, *9*, 899–907.
(12) Velema, W. A.; van der Berg, J. P.; Hansen, M. J.; Szymanski, W.; Driessen, A. J. M.; Feringa, B. L. Optical Control of Antibacterial Activity. *Nat. Chem.* **2013**, *5*, 924–928.
(13) Velema, W. A.; Hansen, M. J.; Lerch, M. M.; Driessen, A. J. M.; Szymanski, W.; Feringa, B. L. Ciprofloxacin–Photoswitch Conjugates: A Facile Strategy for Photopharmacology. *Bioconjugate Chem.* **2015**, *26*, 2592–2597.
(14) Lee, W.; Li, Z.-H.; Vakulenko, S.; Mobashery, S. A Light-Inactivated Antibiotic. *J. Med. Chem.* **2000**, *43*, 128–132.
(15) Eikemo, V.; Sydnes, L. K.; Sydnes, M. O. Photodegradable Antimicrobial Agents − Synthesis, Photodegradation, and Biological Evaluation. *RSC Adv.* **2021**, *11*, 32339–32345.
(16) Eikemo, V.; Holmelid, B.; Sydnes, L. K.; Sydnes, M. O. Photodegradable Antimicrobial Agents: Synthesis and Mechanism of Degradation. *J. Org. Chem.* **2022**, *87*, 8034–8047.
(17) Wan, Peter.; Muralidharan, S. Structure and Mechanism in the Photo-Retro-Aldol Type Reactions of Nitrobenzyl Derivatives. Photochemical Heterolytic Cleavage of Carbon-Carbon Bonds. *J. Am. Chem. Soc.* **1988**, *110*, 4336–4345.
(18) Wan, P.; Muralidharan, S. Photochemical Retro-Aldol Type Reactions of Nitrobenzyl Derivatives. Mechanistic Variations in the Elimination of Nitrobenzyl Carbanions from Nitrobenzyl Derivatives on Photolysis. *Can. J. Chem.* **1986**, *64*, 1949–1951.
(19) Eikemo, V. Synthesis and Photodecomposition Studies of Photodegradable Antibiotics and Chitin Synthase Inhibitors. Ph.D. Dissertation, University of Stavanger, Stavanger, 2021.
(20) Desai, H.; D'Souza, B.; Foether, D.; Johnson, B.; Lindsay, H. Regioselectivity in a Highly Efficient, Microwave-Assisted Epoxide Aminolysis. *Synthesis* **2007**, *2007*, 902–910.
(21) Heydari, A.; Mehrdad, M.; Maleki, A.; Ahmadi, N. A New and Efficient Epoxide Ring Opening via Poor Nucleophiles: Indole, p-Nitroaniline, Borane and o-Trimethylsilylhydroxylamine in Lithium Perchlorate. *Synthesis* **2004**, *2004*, 1563–1565.
(22) Studziński, W.; Gackowska, A.; Przybyłek, M.; Gaca, J. Studies on the Formation of Formaldehyde during 2-Ethylhexyl 4-(Dimethylamino)Benzoate Demethylation in the Presence of Reactive Oxygen and Chlorine Species. *Environ. Sci. Pollut. Res.* **2017**, *24*, 8049–8061.
(23) Bae, D. H.; Shine, H. J. Photobenzidine Rearrangements. 7. Disproportionation and Recombination of N-Methylarylamino Radicals in the Photodecomposition of 1,4-Bis(p-Cyanophenyl)-1,4-Dimethyl-2-Tetrazene and Other 2-Tetrazenes. *J. Org. Chem.* **1981**, *46*, 4700–4704.
(24) Drlica, K.; Zhao, X. DNA Gyrase, Topoisomerase IV, and the 4-Quinolones. *Microbiol. Mol. Biol. Rev.* **1997**, *61*, 377–392.
(25) Coxon, J. M.; Halton, B. *Organic Photochemistry*; Cambridge University Press, 1987.
(26) Lasorne, B.; Worth, G. A.; Robb, M. A. Excited-State Dynamics. *WIREs Comput. Mol. Sci.* **2011**, *1*, 460–475.

(27) Yu, L.; Zhou, W.; Wang, Z. Synthesis and in Vitro Antibacterial Activity of Oxazolidine LBM-415 Analogs as Peptide Deformylase Inhibitors. *Bioorg. Med. Chem. Lett.* **2011**, *21*, 1541–1544.
(28) Faidallah, H. M.; Sharshira, E. M.; Al-Saadi, M. S. M. Synthesis and Biological Evaluation of Some New Alicyclicspiro-2'-(1',3'-Oxazolidine) Derivatives. *Heterocycl. Comm.* **2009**, *15*, 43–50.
(29) Wan, P.; Muralidharan, S.; McAuley, I.; Babbage, C. A. Photooxygenation of Nitrobenzyl Derivatives. Mechanisms of Photogeneration and Hydrolysis of α-Hydroperoxy Nitrobenzyl Ethers. *Can. J. Chem.* **1987**, *65*, 1775–1783.
(30) Forman, M. A.; Dailey, W. P. The Lithium Perchlorate-Diethyl Ether Rate Acceleration of the Diels-Alder Reaction: Lewis Acid Catalysis by Lithium Ion. *J. Am. Chem. Soc.* **1991**, *113*, 2761–2762.
(31) Wang, S.-P.; Chen, H.-J. Separation and Determination of Nitrobenzenes by Micellar Electrokinetic Chromatography and High-Performance Liquid Chromatography. *J. Chromatogr. A.* **2002**, *979*, 439–446.
(32) Zhang, T.; Lang, Q.; Zeng, L.; Li, T.; Wei, M.; Liu, A. Substituent Effect on the Oxidation Peak Potentials of Phenol Derivatives at Ordered Mesoporous Carbons Modified Electrode and Its Application in Determination of Acidity Coefficients (PKa). *Electrochim. Acta* **2014**, *115*, 283–289.
(33) Shin, N. Y.; Tsui, E.; Reinhold, A.; Scholes, G. D.; Bird, M. J.; Knowles, R. R. Radicals as Exceptional Electron-Withdrawing Groups: Nucleophilic Aromatic Substitution of Halophenols Via Homolysis-Enabled Electronic Activation. *J. Am. Chem. Soc.* **2022**, *144*, 21783–21790.
(34) Koudriavtsev, A. B.; Jameson, R. F.; Linert, W. In *The Law of Mass Action*; Springer Science & Business Media, 2001; pp 72 and 137.
(35) Kim, B. H.; Piao, F.; Lee, E. J.; Kim, J. S.; Jun, Y. M.; Lee, B. M. $InCl_3$-Catalyzed Regioselective Ring-Opening Reactions of Epoxides to β-Hydroxy Ethers. *Bull. Korean Chem. Soc.* **2004**, *25*, 881–888.
(36) Fulmer, G. R.; Miller, A. J. M.; Sherden, N. H.; Gottlieb, H. E.; Nudelman, A.; Stoltz, B. M.; Bercaw, J. E.; Goldberg, K. I. NMR Chemical Shifts of Trace Impurities: Common Laboratory Solvents, Organics, and Gases in Deuterated Solvents Relevant to the Organometallic Chemist. *Organometallics* **2010**, *29*, 2176–2179.
(37) National Center for Biotechnology Information. *PubChem Compound LCSS for CID 23108, 2,5-Dichloro-4-nitroaniline*. https://pubchem.ncbi.nlm.nih.gov/compound/23108 (accessed 2023-05-13).

6 Appendix

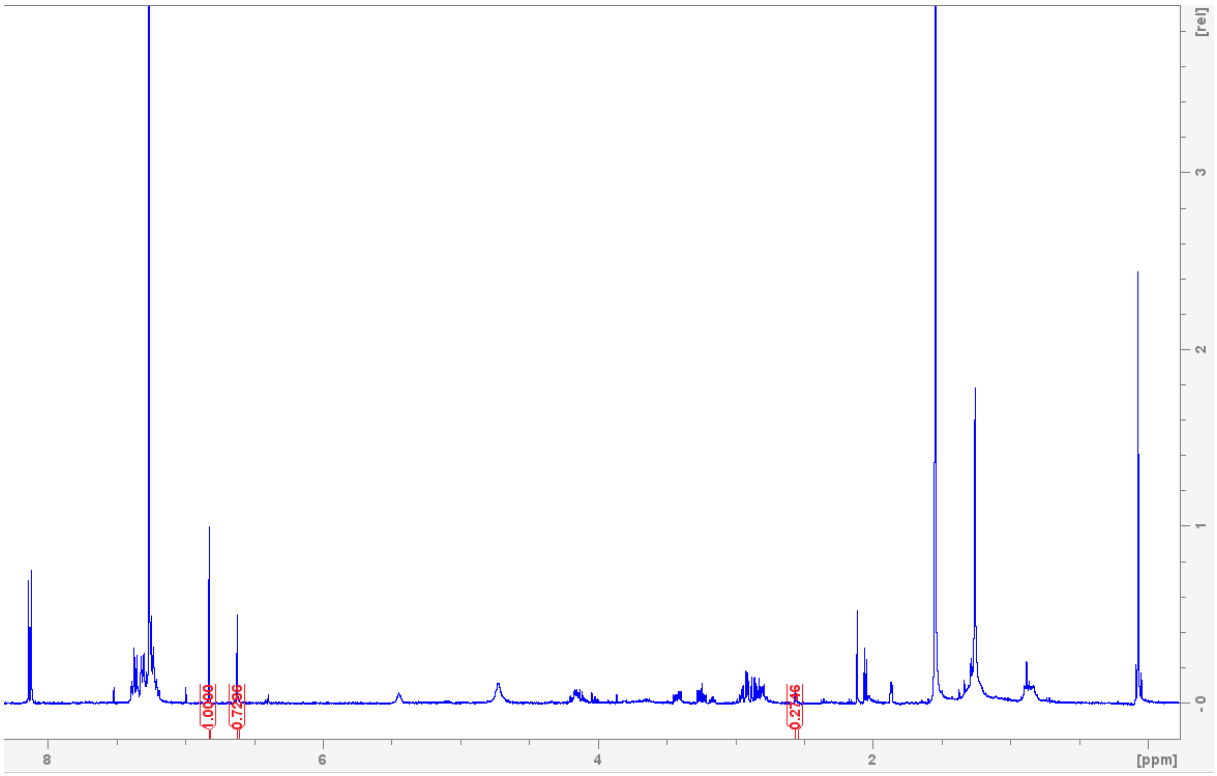

Figure 11. Synthesis of ethanolamine **3a** in 5 M LPEtOAc, second attempt. The ^{1}H NMR specter shows the reaction after 72 h. Peak with integral of 1.00 is aniline **1**; peak with integral of 0.73 is ethanolamine **3a**; peak with integral of 0.27 is epoxide **2**.

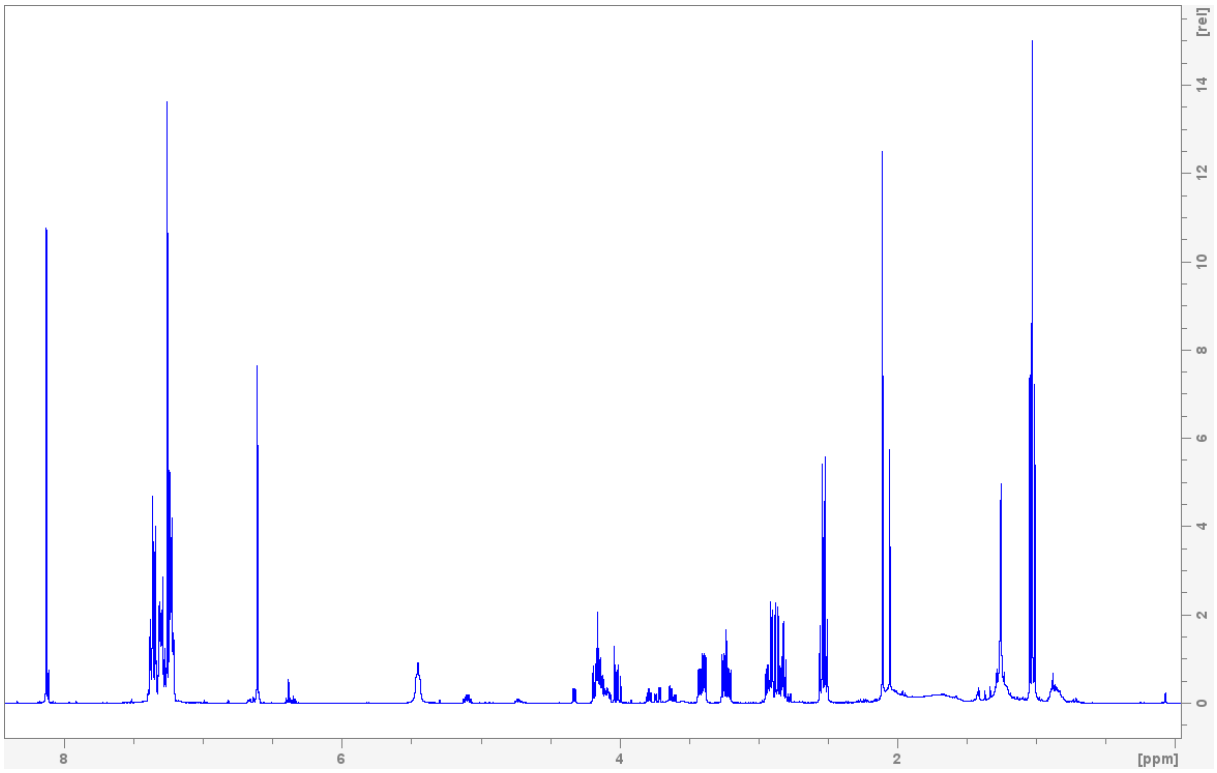

Figure 12. Impure fraction of ethanolamine **3a** used in synthesis of oxazolidine **4**.

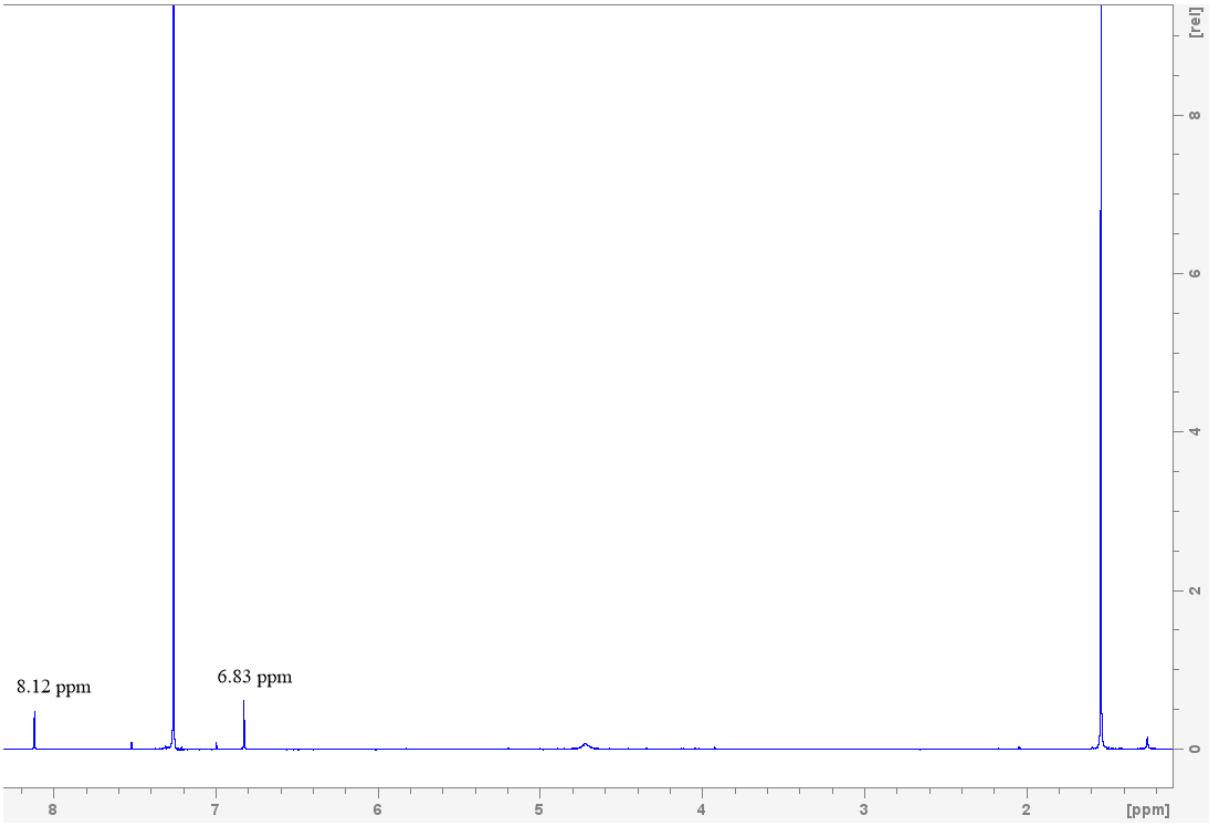

Figure 13. ^{1}H NMR specter of aniline **1a**.

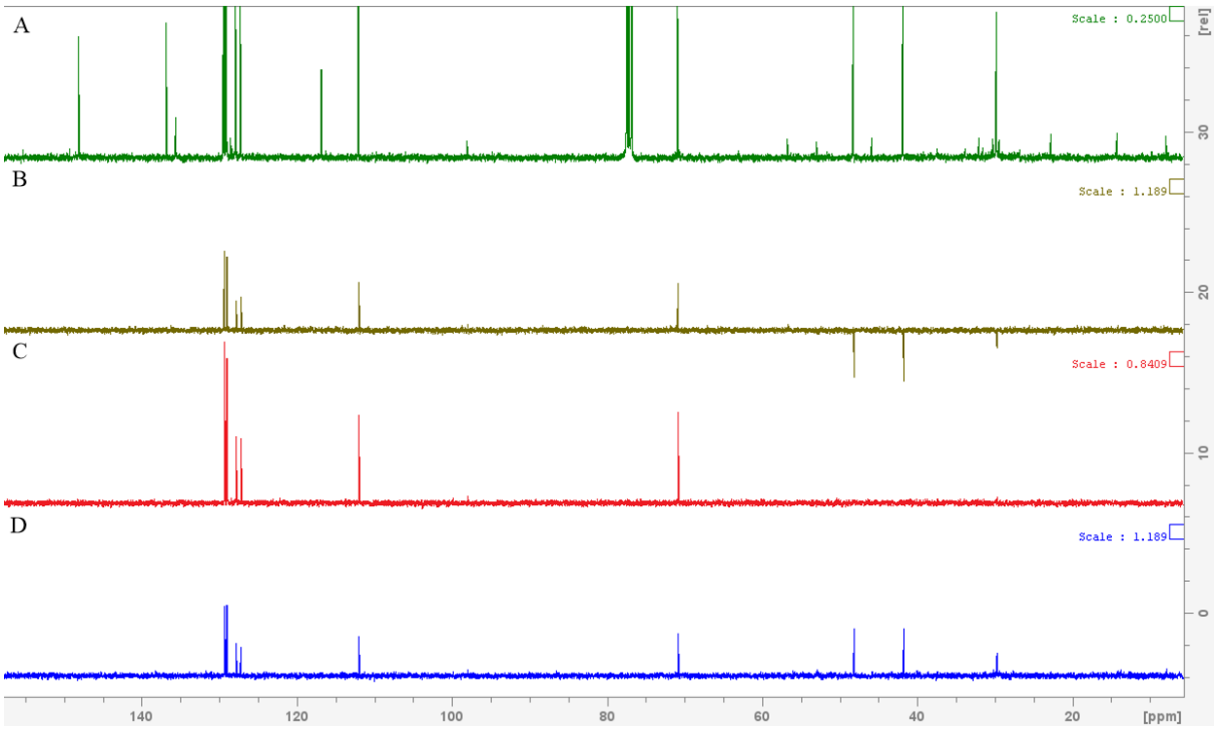

Figure 14. DEPT NMR from synthesis of ethanolamine **3a** in 5 M LPDE. (A) ^{13}C NMR, (B) DEPT-135, (C) DEPT-90 and (D) DEPT-45.

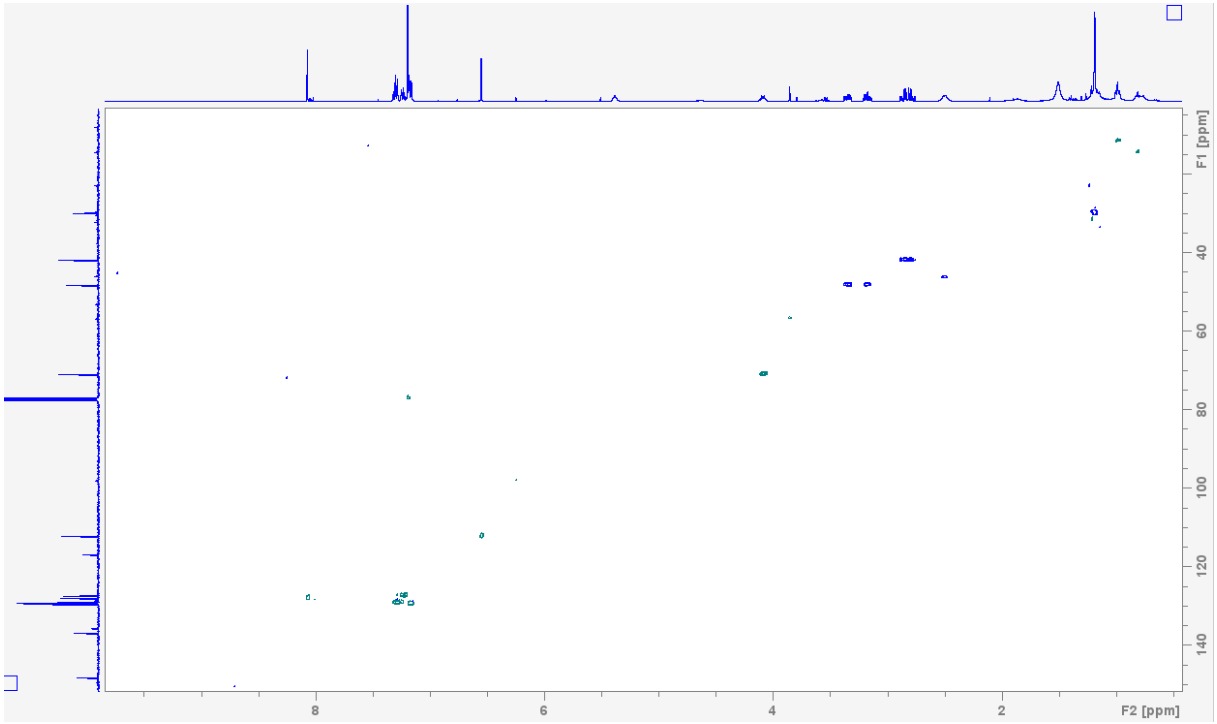

Figure 15. HSQC specter from synthesis of ethanolamine **3a** in 5 M LPDE. The ^{1}H NMR is on the x-axis and the ^{13}C NMR is on the y-axis.

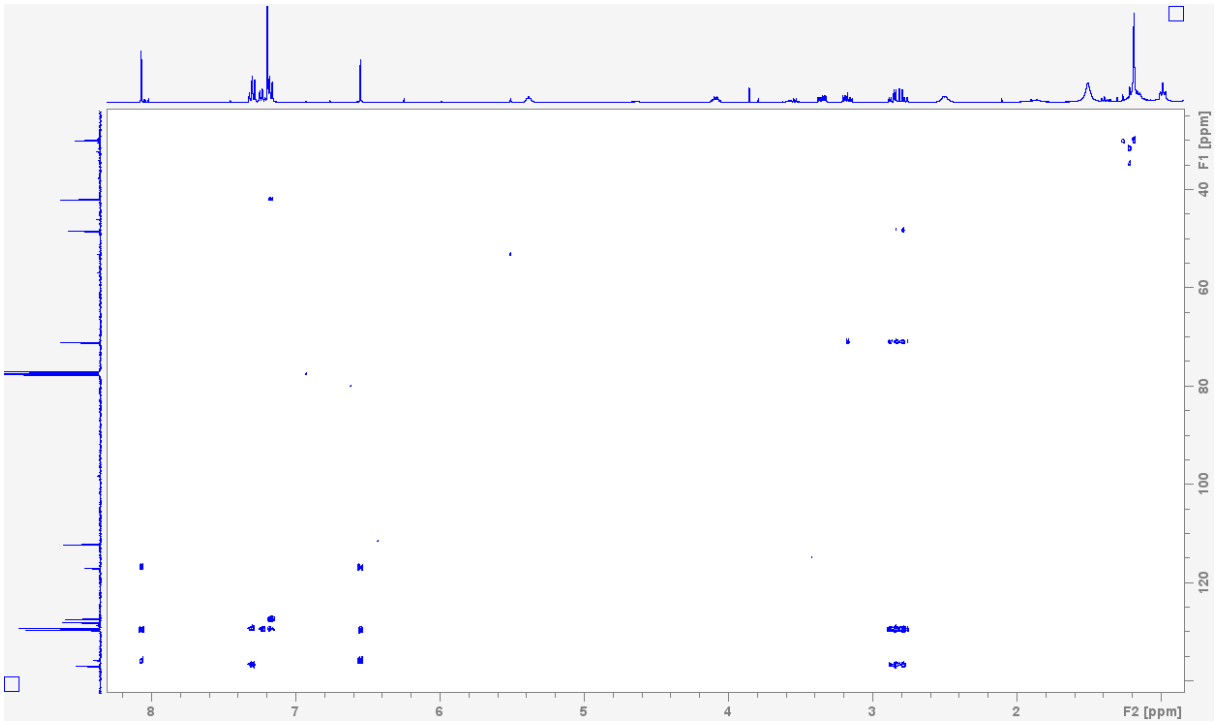

Figure 16. HMBC specter from synthesis of ethanolamine **3a** in 5 M LPDE. The ^{1}H NMR is on the x-axis and the ^{13}C NMR is on the y-axis.

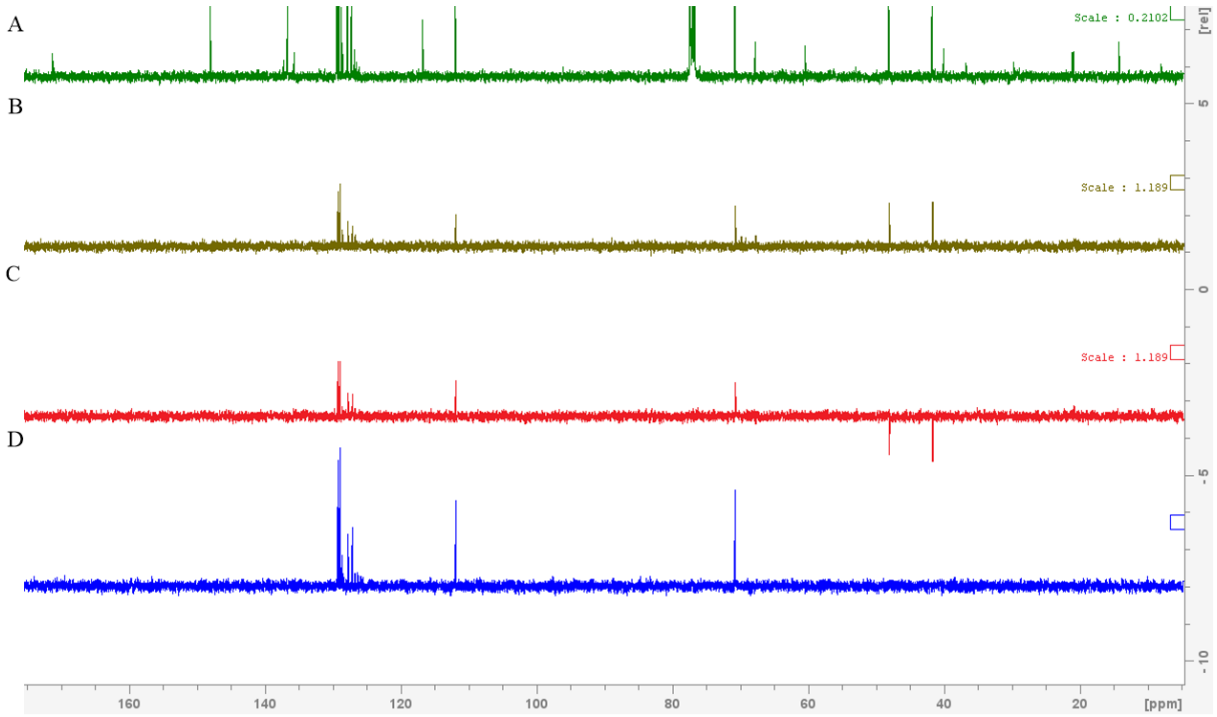

Figure 17. DEPT NMR from synthesis of ethanolamine **3a** in 5 M LPEtOAc, attempt 1 (mixed fraction). (A) ^{13}C NMR, (B) DEPT-45, (C) DEPT-135 and (D) DEPT-90.

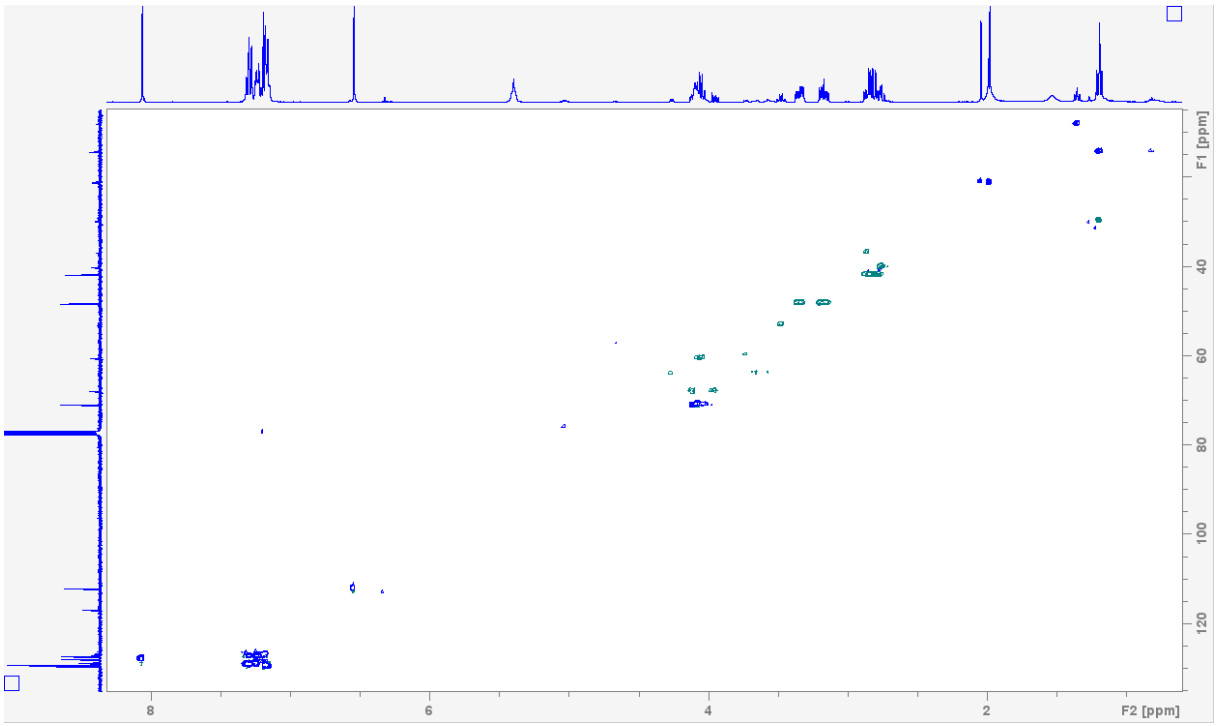

Figure 18. HSQC specter from synthesis of ethanolamine **3a** in 5 M LPEtOAc, attempt 1 (mixed fraction). The ^{1}H NMR is on the x-axis and the ^{13}C NMR is on the y-axis.

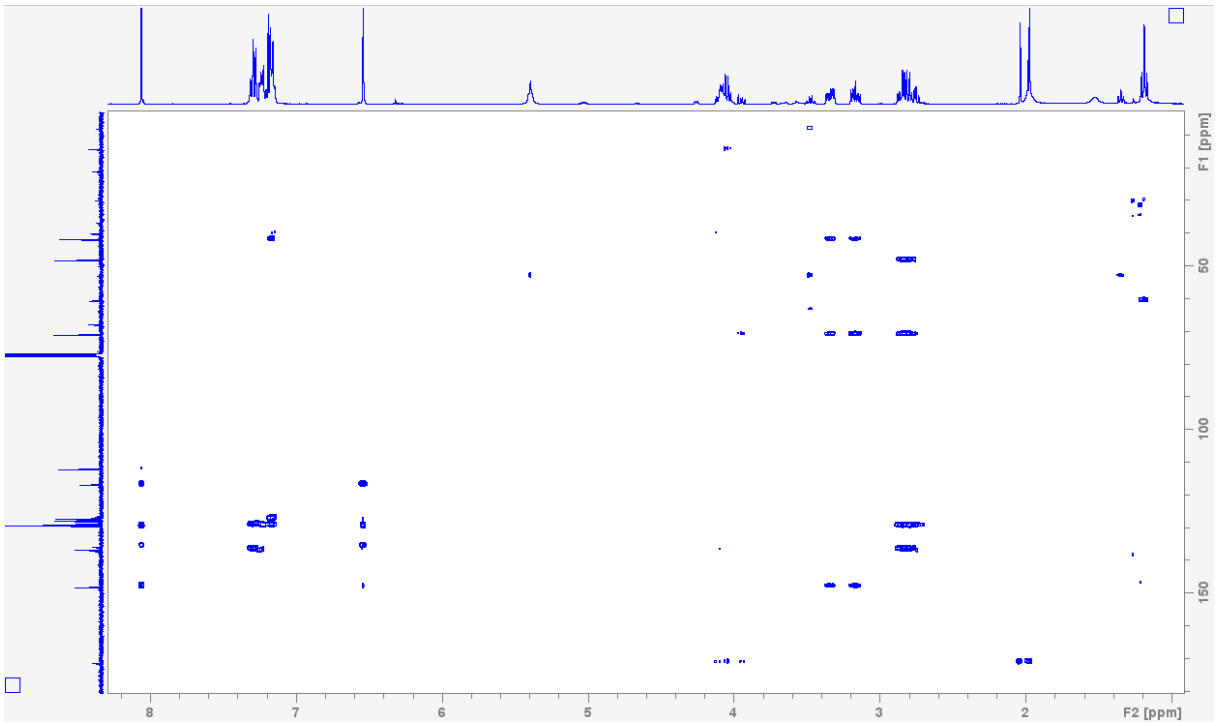

Figure 19. HMBC specter from synthesis of ethanolamine **3a** in 5 M LPEtOAc, attempt 1 (mixed fraction). The ^{1}H NMR is on the x-axis and the ^{13}C NMR is on the y-axis.

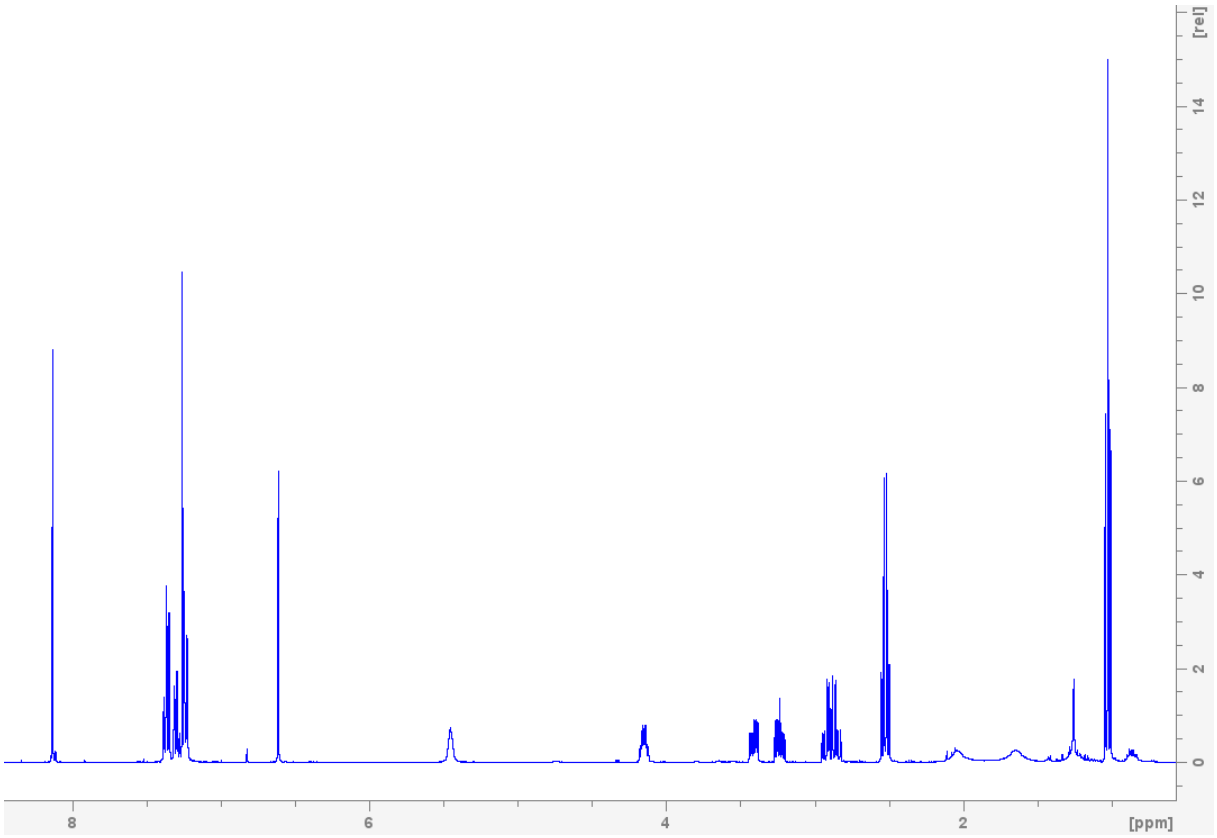

Figure 20. ^{1}H NMR of pure fraction for synthesis of ethanolamine **3a** using 5 M LPEtOAc, attempt 2.

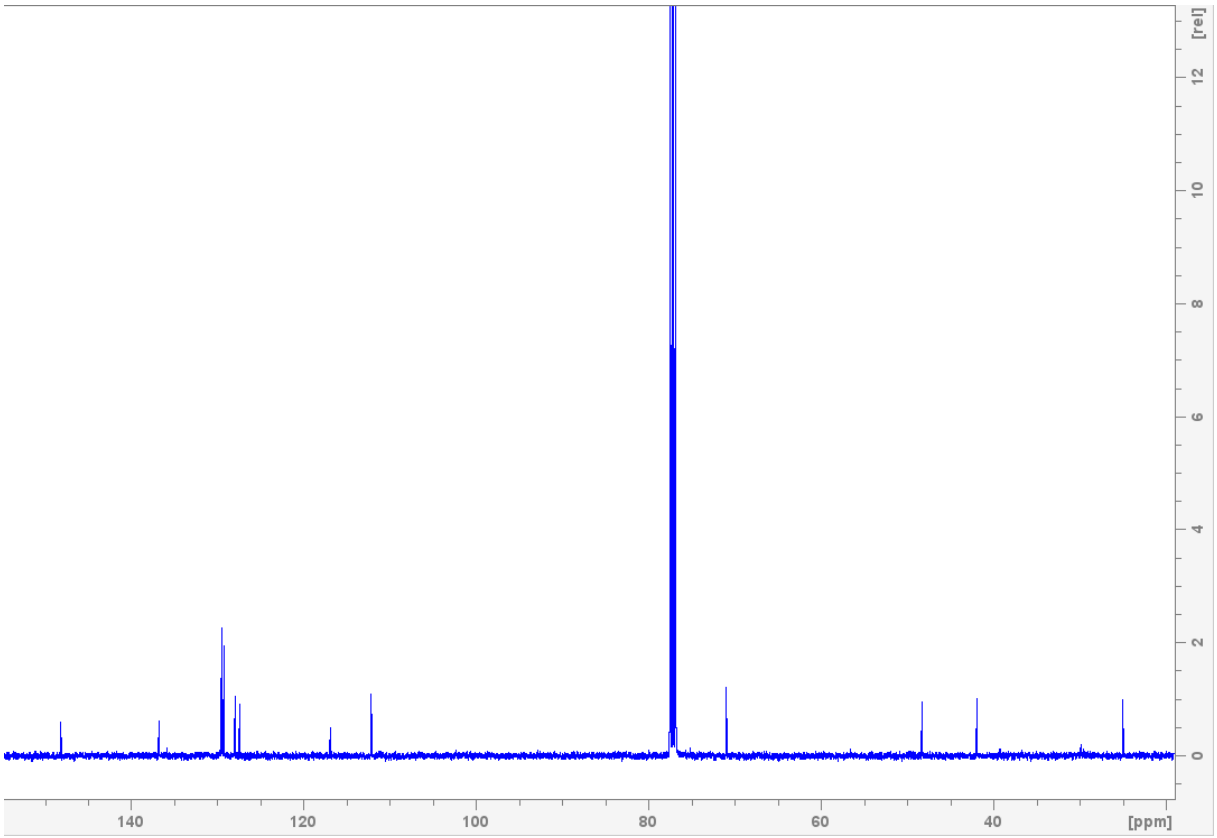

Figure 21. ^{13}C NMR of pure fraction for synthesis of ethanolamine **3a** using 5 M LPEtOAc, attempt 2.

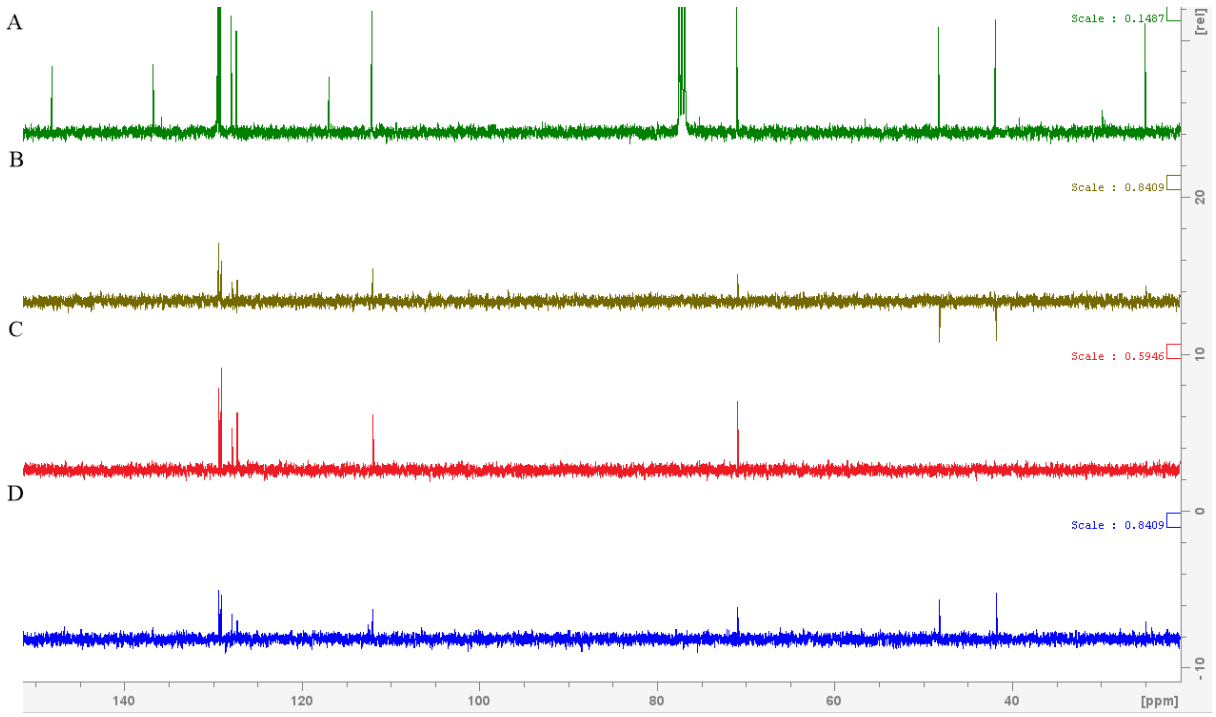

Figure 22. DEPT NMR from synthesis of ethanolamine **3a** in 5 M LPEtOAc, attempt 2. (A) ^{13}C NMR, (B) DEPT-135, (C) DEPT-90 and (D) DEPT-45.

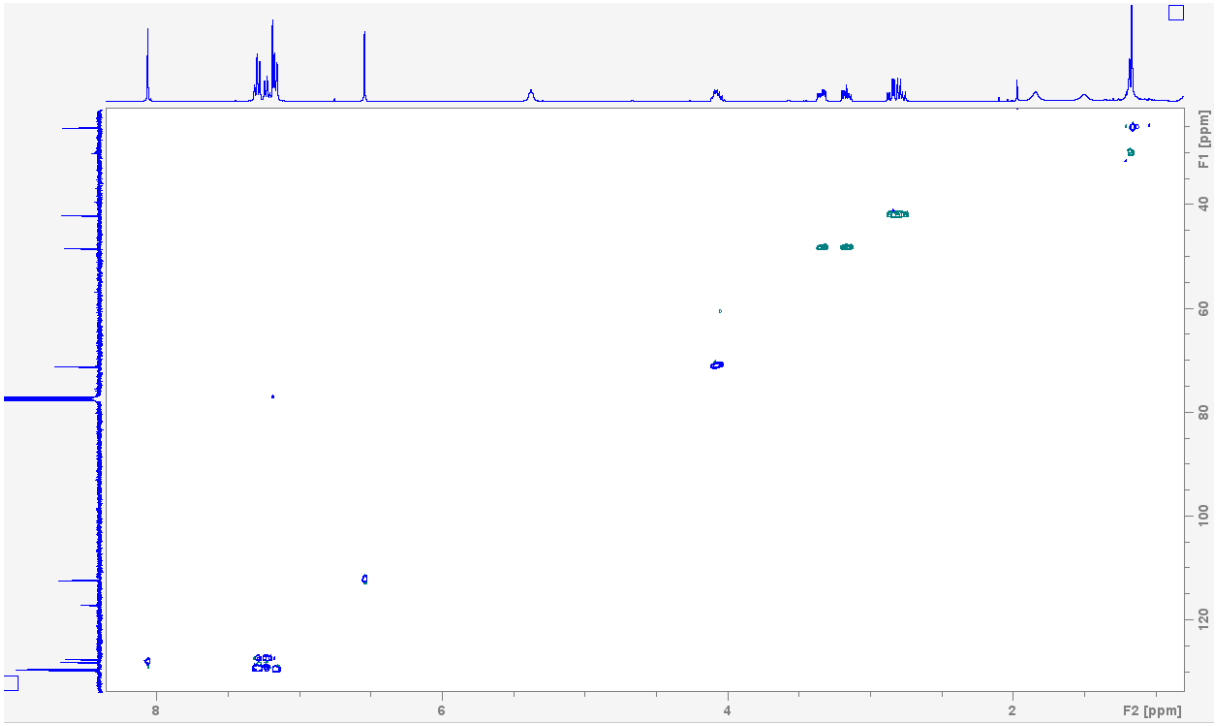

Figure 23. HSQC specter from synthesis of ethanolamine **3a** in 5 M LPEtOAc, attempt 2. The ^{1}H NMR is on the x-axis and the ^{13}C NMR is on the y-axis.

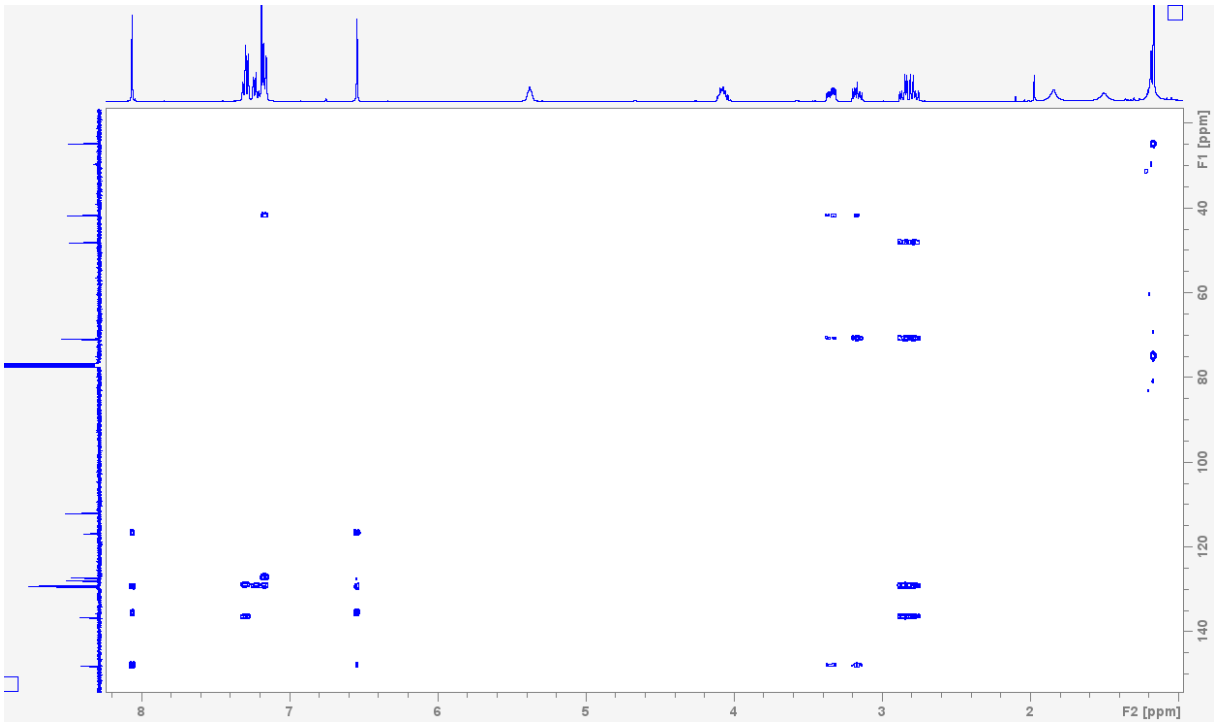

Figure 24. HMBC specter from synthesis of ethanolamine **3a** in 5 M LPEtOAc, attempt 2. The ^{1}H NMR is on the x-axis and the ^{13}C NMR is on the y-axis.

Figure 25. ^{1}H NMR of pure fraction from synthesis of oxazolidine **4**.